Temporal and spatial patterns of biological community development at nascent deep-sea hydrothermal vents (9°50'N, East Pacific Rise)

Timothy M. Shank[a],*, Daniel J. Fornari[b], Karen L. Von Damm[c], Marvin D. Lilley[d], Rachel M. Haymon[e], Richard A. Lutz[a]

[a] *Institute of Marine and Coastal Sciences, Rutgers University, New Brunswick, NJ 08903-0231, USA*
[b] *Department of Geology & Geophysics, Woods Hole Oceanographic Institution, Woods Hole, MA 02543, USA*
[c] *Department of Earth Sciences, University of New Hamphsire, Durham, NH 03824-3589, USA*
[d] *School of Oceanography, University of Washington, Seattle, WA 98195, USA*
[e] *Department of Geological Sciences, University of California at Santa Barbara, Santa Barbara, CA 93106, USA*

Abstract

The April 1991 discovery of newly formed hydrothermal vents in areas of recent volcanic eruption between 9°45'N and 9°52'N on the East Pacific Rise provided a unique opportunity to follow temporal changes in biological community structure from the "birth" of numerous deep-sea hydrothermal vents. In March l992, *DSV Alvin* was used to deploy an on-bottom observatory, the Biologic–Geologic Transect, to monitor faunal succession along a 1.37 km segment of the axial summit caldera between 9°49.61'N and 9°50.36'N (depth ~ 2520 m). Photo- and videographic documentation of megafaunal colonization and chemical analyses of diffuse hydrothermal fluids associated with many of these developing communities within the Transect were performed in March 1992, December 1993, October 1994, and November 1995.

Photographic and chemical time-series analyses revealed the following sequence of events in low-temperature venting areas. (1) Immediately following the 1991 eruption, hydrogen sulfide and iron concentrations in diffuse fluids were extremely high (>1 mmol kg^{-1}) and microbially derived material blanketed active areas of venting in the form of thick microbial mats. (2) Mobile vent fauna (e.g. amphipods, copepods, octopods, and galatheid and brachyuran crabs) and non-vent fauna (e.g. nematocarcinid shrimp) proliferated in response to this increased biological production. (3) Within 1 yr of the eruption, areal coverage of microbial mats

* Corresponding author. Tel.: 001 908 932 8959; fax: 001 908 932 6557; e-mail: shank@imcs.rutgers.edu.

was reduced by $\sim 60\%$ and individuals of the vestimentiferan tube worm *Tevnia jerichonana* settled gregariously in areas where diffuse flow was most intense. (4) Two years after the eruption, maximum levels of H_2S decreased by almost half (from 1.90 to 0.97 mmol kg^{-1}) and dense thickets of the vestimentiferan *Riftia pachyptila* dominated vent openings previously inhabited by *Tevnia jerichonana*. (5) Three years after the eruption, maximum hydrogen sulfide levels declined further to 0.88 mmol kg^{-1} and mussels (*Bathymodiolus thermophilus*) were observed on basaltic substrates. (6) Four years after the eruption, galatheid crabs and serpulid polychaetes increased in abundance and were observed close to active vent openings as maximum hydrogen levels decreased to 0.72 mmol kg^{-1}. Also by this time mussels had colonized on to tubes of *Riftia pachyptila*. (7) Between 3 and 5 yr after the eruption, there was a 2- to 3-fold increase in the number of species in the faunal assemblages. In the absence of additional volcanic/tectonic disturbance, we predict that mytilid and vesicomyid bivalves will gradually replace vestimentiferans as the dominant megafauna 5–10 yr following the eruption. We also anticipate that the abundance of suspension feeders will decline during this period while the abundance of carnivores will increase. We hypothesize that the above series of events (1–7) represents a general sequence of biological successional changes that will occur at newly formed low-temperature deep-sea hydrothermal vents along the northern East Pacific Rise and contiguous ridge axes.

Megafaunal colonization at deep-sea hydrothermal vents is considered to be the consequence of an intimate interaction of the life-history strategies of individual species, physical oceanographic processes, and the dynamic hydrothermal environment. Our observations indicate that the successful sequential colonization of dominant megafaunal vent species, from *Tevnia jerichonana* to *Riftia pachyptila* to *Bathymodiolus thermophilus*, also may be strongly influenced by temporal changes in geochemical conditions. Additional evidence demonstrating the close link between diffuse vent flux, fluid geochemistry, and faunal succession included the rapid death of several newly formed biological assemblages coincident with abrupt changes in the geochemical composition of the venting fluid and the local refocusing or cessation of vent flow. These correlations suggest that future models of faunal succession at hydrothermal vents along intermediate to fast-spreading mid-ocean ridges should consider not only the interplay of species-specific life-history strategies, community productivity, and physical oceanographic processes, but also the influence of changing geochemical conditions on the sequential colonization of megafaunal species.

1. Introduction

In many space-limited marine communities, abiotic disturbance events are key structuring forces (Connell, 1979; Sousa, 1980; Keough, 1984; Pickett and White, 1985). Studies investigating the re-establishment and development of communities after natural, large-scale catastrophic disturbances have been limited largely to terrestrial ecosystems following volcanic eruptions [e.g. Anak Krakatau Island (Bush and Whittaker, 1991; Thornton and Walsh, 1992), Mount St. Helens (Dale, 1991), Pitcairn Island (Diamond, 1994), and Surtsey Island (Fridriksson and Magnusson, 1989)]. Hydrothermal vent habitats in the deep ocean also experience large-scale catastrophic events. Frequent volcanic eruptions and tectonic disturbance (Haymon et al., 1993; Embley et al., 1995), as well as inherently unsteady vent fluid convection through young oceanic crust (Watremez and Kervevan, 1990), create highly variable,

transient habitats. Understanding the processes by which deep-sea hydrothermal vent-endemic species successfully establish and maintain communities in patchily distributed, ephemeral habitats has been a fundamental goal of hydrothermal vent ecology (Tunnicliffe, 1991). The April 1991 discovery of newly formed hydrothermal vents in volcanically active areas of the fast-spreading (11–12 cm yr^{-1}; Carbotte and MacDonald, 1992) East Pacific Rise (EPR) between 9°45′N and 9°52′N (Haymon et al., 1993) presented a rare opportunity to document the colonization of newly formed vents, examine the chemical, geological, and oceanographic processes that impact community establishment, and define time-scales over which communities develop, undergo structural/faunal changes, and eventually die. Additionally, this event afforded the opportunity to assess existing hypotheses of faunal succession at deep-sea hydrothermal vents (Hessler et al., 1988; Fustec et al., 1987; Jollivet, 1993) and develop new descriptive models.

Most previous studies of temporal and spatial change in mid-ocean ridge (MOR) vent communities have been conducted without knowing the age of the existing community relative to the inception of hydrothermal activity caused by volcanic and tectonic activity (e.g. Fustec et al., 1987; Hessler et al., 1988; Johnson and Tunnicliffe, 1988; Tunnicliffe and Juniper, 1990; Tunnicliffe et al., 1990). Attempts to relate the relative age of lava flows to faunal composition have been conducted by Milligan and Tunnicliffe (1994) along the Cleft segment, Juan de Fuca Ridge, and Geistdoerfer et al. (1995) and Auzende et al. (1994) along the southern EPR. The relative age of biological communities and the initiation of venting at certain vent sites at 13°N EPR also have been inferred from records of seismic activity by Jollivet (1993). During the past 7 years, three submarine eruptions and the accompanying onset of hydrothermal activity have been documented on the MOR: (1) along 9°–10°N EPR in 1991 (Haymon et al., 1993; Gregg et al., 1996); (2) at CoAxial Seamount of the Juan de Fuca Ridge in 1993 (Delaney and Embley, 1993; Embley et al., 1995; Tunnicliffe et al., 1998); and (3) along the northern Gorda Ridge near 42°40′N in 1996 (Embley et al., 1996). Anthropogenically induced venting brought about by deep-drilling at Middle Valley (Holden, 1996) and the recent eruption of Loihi Seamount (Duennebier et al., 1997) represent other fortuitous events that provide opportunities for further study of the natural development of vent-endemic faunal communities.

Over the past 15 years, observations during repeat visits to eastern Pacific vent sites indicate that well-established biological vent communities undergo substantial changes in their composition and distribution (Fustec et al., 1987; Hessler and Smithey, 1983; Hessler et al., 1985; Hessler et al., 1988; Tunnicliffe et al., 1990; Van Dover and Hessler, 1990; Jollivet, 1993). Wholly or partially dead beds of clams (*Calyptogena magnifica*) observed at 21°N EPR between 1982 and 1990 attest to the effect discontinuous vent emission can have on biological communities (Lutz, 1991; Fisher et al., 1988). The abundance of *Riftia* at 21°N was virtually eliminated by intensive research sampling in 1982, but dramatically increased by 1990 (Lutz, 1991). Vent sites near 13°N EPR experienced periods of marked instability in venting activity between 1982 and 1990 (Jollivet, 1993). Inactive periods of venting were characterized by a sharp decrease in *Riftia* populations, an increase in scavengers, and a persistence of mytilid bivalves (*Bathymodiolus thermophilus*). Reactivation of extinct vent areas was

correlated with increased numbers of *Tevnia jerichonana* and *Bythograea thermydron* (Jollivet, 1993). Under seemingly constant venting conditions at Rose Garden vents (Galápagos Rift) from 1979 to 1990 (Hessler and Desbruyères, 1991), the abundance of *Riftia* declined sharply and was replaced with the mytilid *B. thermophilus* and the vesicomyid *C. magnifica.* At the Mushroom Vent site on Axial Seamount along the Juan de Fuca Ridge, the natural development of vestimentiferan communities was significantly altered by organism sampling and the excavation and removal of sulfides (Tunnicliffe and Juniper, 1990). It thus appears that the spatial readjustment of vent emissions, altered intensity of fluid flux, and the physical effects of tectonic perturbations and anthropogenic disturbance can have dramatic effects on the temporal and spatial variation in vent community structure. These studies also demonstrate that dramatic faunal changes can be observed over periods of several years, although distinguishing between naturally occurring faunal changes and the effects of anthropogenic disturbance (e.g. extensive sampling, manipulative experiments, and submersible maneuvering) can be extremely difficult (Tunnicliffe, 1990).

In this study our main goals are to: (1) document the temporal sequence of species colonization and dominance within spatially separated low-temperature faunal communities; (2) assess the rate at which various species colonize new vents; (3) correlate changes in community composition with changes in diffuse vent fluid flux and geochemistry; and (4) develop a descriptive model of vent faunal "succession" along certain intermediate- to fast-spreading MORs in the eastern Pacific. In order to accomplish these goals, we established a long-term study area for monitoring seafloor processes between 9°49.61′N and 9°50.36′N on the EPR crest (Fig. 1). This area, termed the Biologic–Geologic Transect (Transect), extends along a 1.37 km long section of the floor of the axial summit caldera (ASC) and traversed seven high-temperature vents and at least 17 areas of low temperature, diffuse flow that formed during the 1991 eruption. Photographic and videographic images were obtained 15 months prior to the eruption, and 2 weeks, 11 months, 32 months, 42 months, and 55 months after the eruption in order to document temporal changes in biological community structure. In addition to the extensive photographic and videographic images, concomitant time-series measurements and analyses of low-temperature diffuse vent fluid chemistry and temperature permitted correlation of abiotic factors with observed changes in community structure.

2. Methods

2.1. Study area

The following considerations were used in selecting the region between 9°49.61′N and 9°50.36′N as the Transect area: (1) a November 1989 photosurvey (conducted using the deep-towed vehicle *Argo*) identified this area of the EPR crest as one of the most hydrothermally active segments between 9°09′N and 9°54′N, (Haymon et al., 1991) with well-developed vent communities between 9°45′N and 9°51′N; (2) in April 1991, venting in the area between 9°49.61′N and 9°50.36′N ranged from
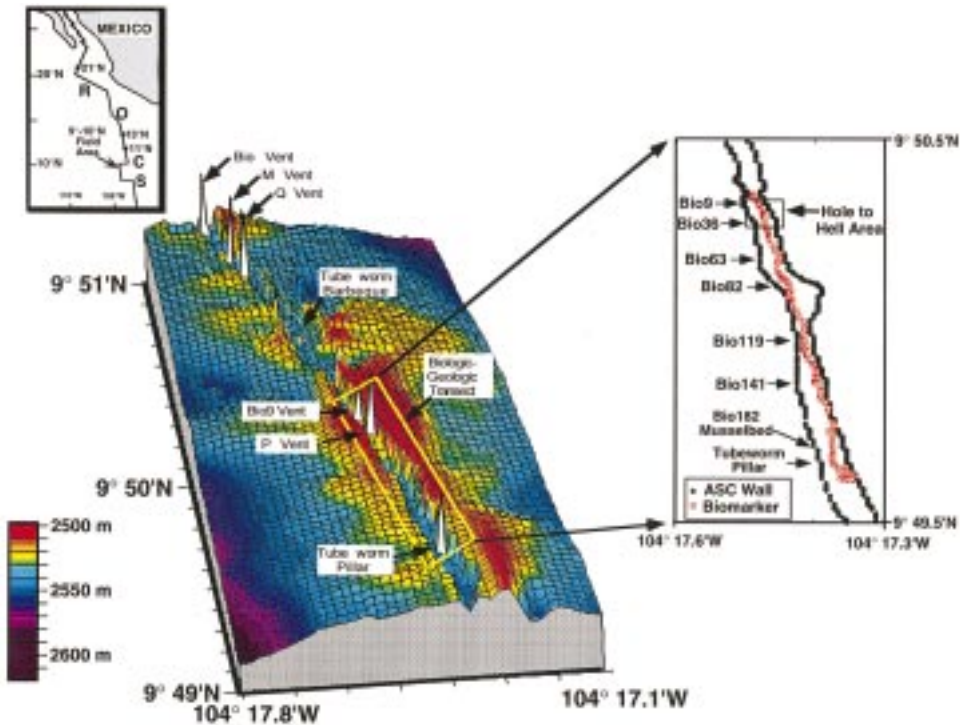
Fig. 1. Bathymetric map of the East Pacific Rise ridge crest between 9°49′N and 9°51′N indicating the location of the 1.37 km long Biologic–Geologic Transect (yellow boxed area) and principal high temperature vents (shown in white and vertically exaggerated) in this region. Grid (interval = 20 m) constructed from *Alvin* altitude and depth, and corrected Sea Beam depth data. Inset (top left) shows the location of the 9°–10° North field area between the Clipperton (C) and Siquieros (S) Transform Faults, and other EPR vent fields located at 21°N, 13°N, and 11°N, with the Rivera (R) and Orozco (O) Transform Faults separating these sites. Map (at right) depicts the positions of the 210 Biomarkers of the Biologic– Geologic Transect deployed along nascent and pre-eruption vent areas within the axial summit caldera (ASC) between 9°49.61′N and 9°50.36′N in March 1992. Red squares and black diamonds indicate the relative positions of the Biomarkers and the walls of the axial summit caldera, respectively. The "Hole-to-Hell" (black box) area is bounded by two areas of high-temperature venting ("Bio 9" and "P vent"). Arrows indicate locations of biological colonies, as well as two pre-eruption communities (Bio182 Musselbed and the Tube Worm Pillar) whose development has been documented since the April 1991 eruption.
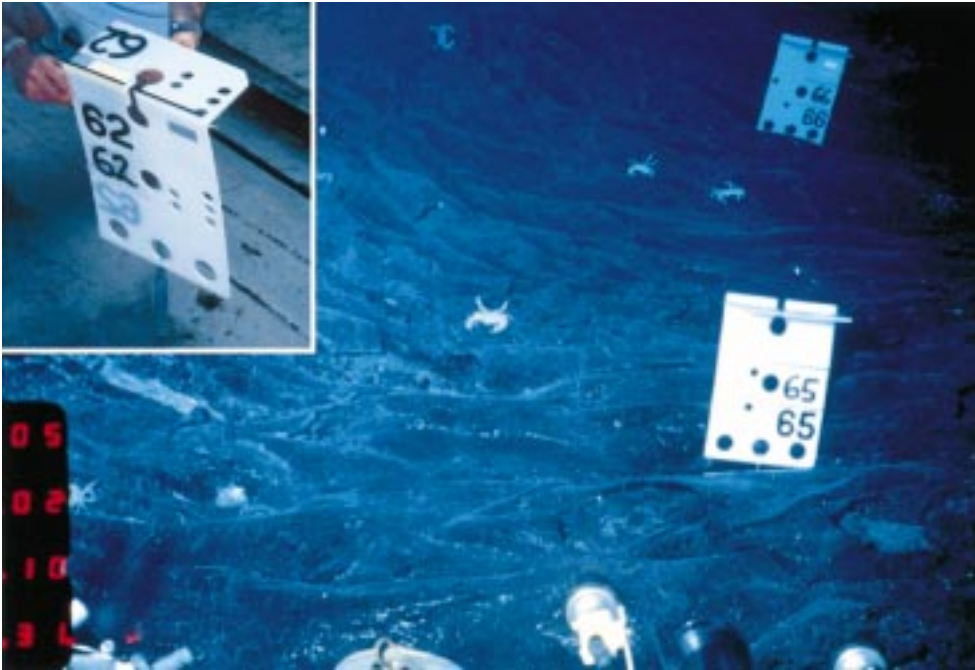
Fig. 2. Polyethylene "Biomarkers" deployed along the axial summit caldera floor. Each Biomarker consisted of a vertical polyethylene panel (45 cm × 30 cm × 1 cm) and an attached, horizontal overhanging polyethylene "flap" (15 cm × 30 cm × 1 cm). Analog numbers (1–210), an optically readable eight-bit binary code system (consisting of 2.5 cm holes, recognizable in the event of fouling), and reflective and phosphores-cent tapes were employed to facilitate Biomarker recognition by a variety of submersible systems. In order to stabilize the on-bottom position, each Biomarker was weighted with a 0.5 kg stainless steel anchor bar with a swivel that permitted rotation of the marker in the presence of currents and submersible propwash. Inset shows Biomarker #62 on the deck of the *R/V Atlantis II*.

high-temperature (392°C) fluids emanating from orifices in bare basalt (with little or no associated sulfide deposits) to clouds of diffuse flow issuing from fissures, cracks, and deep pits of collapsed lava. The fresh lava flows and numerous nascent hydrothermal vents were covered with thick microbial material with a notable absence of megafauna; (3) in March 1992, newly established vent-endemic invertebrates were found inhabiting these same areas of diffuse venting.

2.2. Transect installation

In March l992, 210 polyethylene markers, referred to as Biomarkers (Fig. 2), were deployed from *Alvin* at intervals ranging from ∼ 1 to 15 m along the Transect. Attempts to space the Biomarkers farther apart in less hydrothermally active areas and closer together in areas of intense venting activity were made along the length of the Transect (see Fig. 3). The Biomarkers provide benchmarks that unequivocally locate meter-scale areas in which temporal change can be characterized quantitatively. In order to assess the extent to which Biomarkers moved, we installed a fixed marker with a 3–5 kg anchor immediately adjacent to five Biomarkers at various intervals along the Transect. Since the establishment of the Transect, these Biomarkers have not moved with respect to their paired fixed marker. A few Biomarkers located on the margins of fissures, or on the rims of collapse pits, have shifted position due to the collapse of lobate lava surfaces.

Biomarkers were deployed and surveyed during *Alvin* dives 2496, 2499, and 2501. The location of each Biomarker was determined to within 2–4 m in geodetic coordinates by acoustic ranging from *Alvin* to a permanently-moored, long-baseline acoustic navigation system. Transponders were surveyed acoustically using global positioning system (GPS) data; root mean square errors of transponder positions were 1.1 m. During dive 2504, *Alvin* continuously surveyed the Transect by traversing at an altitude of 1–4 m over the Biomarkers in a north to south direction at a constant speed of ∼ 12 m/min.

2.3. Photographic documentation

Photographic surveys. Photographic surveys were conducted near or within the Transect area during six cruises between 1989 and 1995 (Fig. 1). Image data collected between 1989 and 1992 consisted of sporadic 35 mm photographs, color video recorded on VHS, 8 mm or Hi-8 tape, and black and white video from a wide-angled silicon-intensified target (SIT) camera. From 1993 to 1995, imaging capabilities improved with the use of metal-halide lighting (developed by M. Olsson and Deep-Sea Power and Light) and a high-resolution color 3-chip charged-couple device (CCD) video system (developed by W. Lange and Woods Hole Oceanographic Institution) recorded to a broadcast-quality Betacam SP format. The 3-chip CCD camera (capable of 750 lines of television resolution) was equipped with a zoom lens with a focal length of 5–47 mm providing abundant, high-quality images that could be digitally scanned, thereby facilitating accurate reproduction of precise azimuths and positions of observations made at many sites along the Transect. Scaling of animals
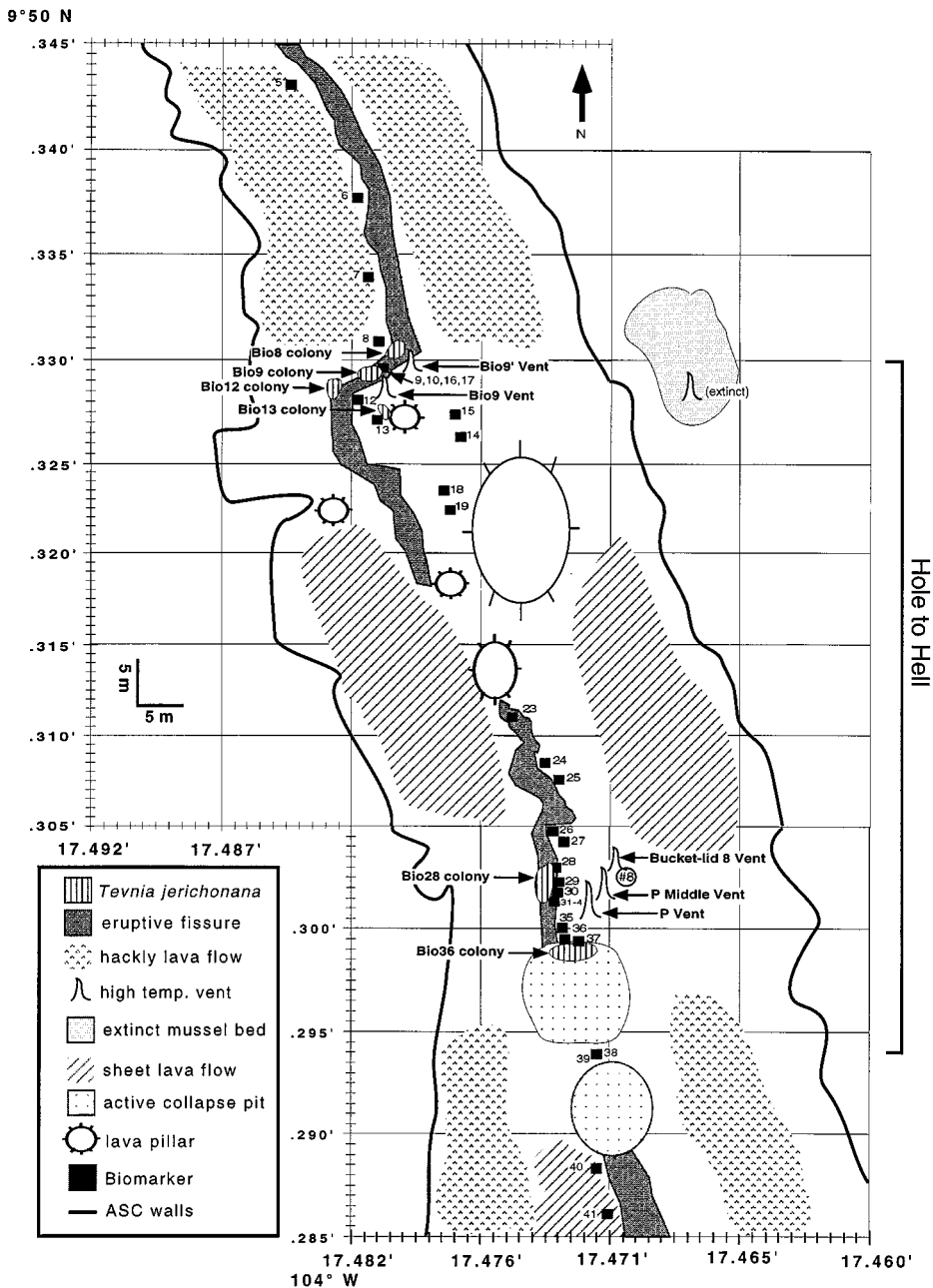
Fig. 3. Map of the northern Transect region between 9°50.285′N and 9°50.345′N (a 120 m distance) featuring the location of the six vestimentiferan colonies (as they appeared in March 1992) in close proximity to five high-temperature vents along the central primary eruptive fissure within the Hole-to-Hell area. Unlabeled lava flow types on the ASC floor are areas where flows are a jumbled mixture of adjacent flows. Axis tick = 1 m.

and features within images was essential to estimating organism size, abundance, and area occupied on the seafloor. The 3-chip camera was fitted with four, orthogonally mounted 635 nm red-orange micro-lasers to provide quantitative scale within images (Tusting and Davis, 1992). Three of the lasers were parallel to the optical axis of the camera, while the fourth laser was pointed at an angle such that its beam converged with its opposing laser at exactly 2 m distance in water. Calibration and confirmation of this laser configuration was performed using a 50 cm^2 grid placed 2 m from the camera lens by *Alvin*'s manipulator claw at a depth of ∼ 200 m as the submersible descended through the water column. This multi-beam laser scaling array permitted the determination of object size, as well as the distance from the camera to the object on the seafloor (Tusting and Davis, 1992; 1993). Additionally, Biomarkers imaged adjacent to animal communities were used as a check on the accuracy of quantitative laser measurements.

Enumeration of "Colonies". We refer to discrete vent areas containing developing vestimentiferan populations (and subsequent colonizers) as "colonies" which are identified by the nearest Biomarker number (e.g. Bio9 and Bio141; Fig. 3). The 3-chip camera was mounted on the *Alvin*'s basket or on the starboard manipulator arm and positioned parallel to the submersible's long axis. At each colony, video images were collected at a minimum of three pre-determined headings at a variety of focal lengths. Far-field and vertical-incidence (down-looking) imaging (4–8 m from the subject plane) also was conducted to determine the area occupied by the colony, and close-up macro-scale imaging (1–2 m from subject, full zoom) allowed size and abundance determination of individual species. Three to five video frames covering at least three different headings at each developing vent colony were captured digitally using Media Cybernetics Image Pro-Plus software and a Coreco Oculus-TCX/MX image capture board. From the positions of the laser dots within each digital image, perspective and vertical grids were constructed and overlaid on the image. Direct counts of individual organisms and determination of area within the field of view were obtained using methods previously described by Tusting and Davis (1993).

The pre-determined submersible headings from which video images were recorded were selected to minimize topographic relief and reduce the error inherent with the assumption of a flat seafloor in perspective grid analysis. Additional error in quantitative estimates of seafloor area and vestimentiferan abundance was introduced by the variation in thickness of individual tube worm assemblages, which increased over time. Average variability of estimates obtained from images of vestimentiferan colonies ranged from ± 15 individuals (in colonies under ∼ 150 ind.) to ± 95 individuals (in colonies exceeding ∼ 800 individuals) or 10–12%. For individual size determination, accuracy varied widely, depending on the taxa imaged. Among tube worms, the frequent inability to adequately observe the point at which the posterior end of the tube was in contact with substrate prevented accurate determination of tube length in ∼ 90% of the individuals within a given colony. For tube worms for which the entire tube was visible, estimates varied ± 3 cm, depending on the oblique angle of the camera and the angular position of the posterior end. The variability in the diameter of the laser spot on the seafloor had little effect on quantitative estimates, as spot

diameter ranged from 0.5 to 1.5 cm, depending upon the focal distance and the intensity of shimmering vent fluids.

Strip transect surveys. Strip transect surveys (McCormick and Choat, 1987; Buckland et al., 1993) were conducted using *Alvin* by traversing over Biomarkers from north to south at 12 m min^{-1}. The 3-chip camera was positioned at an oblique ($\sim 40°$) angle 3–6 m above the seafloor during transect surveys to determine gradients in the distribution of mobile and sessile megafauna over time. Transect runs were conducted at the beginning and end of each dive program in December 1993, October 1994, and November 1995. Scoring of identifiable mobile organisms was performed every 3–7 s of continuous video. Seafloor area was determined using horizontal and vertical laser distance every 12–17 s of continuous video data (equating to $\sim$ 3–15 m of linear seafloor distance), depending on laser visibility. Running averages of seafloor area were computed and the number of organisms per square meter determined. Computer-generated maps (Fig. 3) delineating the spatial distribution of biological and geological features along the length of the Transect were constructed by integrating Biomarker position, submersible navigation, and prominent topographic features in the ASC during each field program.

Vent fluid chemistry. Diffuse vent fluids were sampled from low-temperature faunal communities using the NOAA manifold water sampler (Massoth et al., 1988) equipped with both "major" and "gas tight" titanium water samplers in April 1991, December 1993, October 1994, and November 1995 (Von Damm et al., 1994; Von Damm et al., 1996; Lilley et al., 1996). Sampling locations within developing communities were within $\sim$ 1.5 m in successive years. During field programs in 1993, 1994, and 1995, two to ten discrete water samples were obtained from within these communities and subsequently analyzed using methods described in Von Damm et al. (1997) to determine the chemical composition and concentration of numerous chemical species including hydrogen sulfide, iron, carbon dioxide, methane, magnesium, chloride, and silica. In each case, the manifold intake wand was carefully positioned at the base of vestimentiferan tubes. Extreme care was taken during water sampling to ensure minimal disturbance to the surrounding biological communities. Temperatures of diffuse fluids were monitored during each field program using the *Alvin* temperature probe and manifold intake wand, and between field programs since December 1993 using self-recording, time-lapse temperature (HOBO^{TM}) probes (Fornari et al., 1994; Shank et al., 1995).

3. Results

3.1. Geologic and hydrothermal setting

The physical characteristics of the ASC between 9°09′N and 9°54′N and relationships to hydrothermal vent distribution, faults, and fissures are described by Fornari et al. (1990), Haymon et al. (1991, 1993), Fornari and Embley (1995), Wright et al., (1995), and Fornari et al. (1998). In plan-view the ASC outline is sinuous (Figs. 1 and 3), and its width in the 9°49′–51′N region varies between 40 m, near 9°50.8′N, and 110 m,

just north of 9°49.0′N. The height of the ASC walls within the Transect area varies from ∼ 5–8 m. In places, the wall consists of irregular stair-steps with one or two narrow (1–3 m wide) benches formed by apparent still-stands of lava that represent eruptions which partially filled the ASC locally. Lava pillars (2–8 m high) commonly support archways of uncollapsed roof sections of ponded lava flows along the margins and the floor of the ASC (Fig. 4a and b).

Between 9°49′ and 9°51′N, the primary eruptive fissure inferred to have fed the 1991 eruption (Haymon et al., 1993; Gregg et al., 1996) can be followed nearly continuously over distances of hundreds of meters. This fissure often comprises an anastomosing single crack ∼ 1–3 m wide and ∼ 2–5 m deep, which cuts across hackly, sheet and ponded flows in the ASC floor (Fig. 4c). The location of the fissure within the ASC is nearly coincident with the line of Biomarkers (Fig. 1). Based on field relationships observed between April 1991 and November 1995, considerable post-volcanic modification has influenced the current plan-view geometry of the fissure. This modification is principally manifested in the variable collapse of lava crusts along the fissure margin, short (∼ 5–20 m) offsets of the primary fissure (e.g. at Bio9 vent, Fig. 3), and occasional short parallel cracks or elongate collapse depressions. A region of extensively collapsed lobate lavas was also present along the length of the Transect in a zone ∼ 50–200 m wide on the ASC margin (Fig. 4b). This large-scale porosity and permeability offers great potential for circulating hydrothermal fluids and harboring subsurface microbial communities.

The Transect was divided into eight regions in order to characterize the distribution of biological communities, hydrothermal setting, and lava morphology (Table 1). Nascent hydrothermal venting and incipient biological colonization occurred between Biomarkers #1 and #160. This ∼ 1.02 km region within the Transect was chosen as the primary area for studying vent community development and has been termed the "Phoenix" vent site. Between Biomarkers #160 and #210, there were two areas in which extensive communities existed prior to the 1991 eruption: a basalt/sulfide edifice known as "Tube Worm Pillar" (an 11 m high structure covered by an extremely large population of *Riftia pachyptila*), and a ∼ 20 × 50 m bed of mytilid bivalves (*Bathymodilus thermophilus*) and serpulid polychaetes (*Laminatubus alvini* and *Protis hydrothermica*). The proximity of both nascent and previously established biological communities in the Transect provided the ability to monitor changes in early and mature stages of community development in spatially proximal areas.

Within the Transect there were four areas (each less than 40 m^2) of high-temperature venting (>350°C). High-temperature vents activated as a result of the 1991 eruption are near Biomarker #9 (Bio9 Prime vent and Bio9 vent) and Biomarker #35 (P vent, P Middle vent, and Bucket-lid 8 vent) (Fig. 3). Two areas of focused flow, present prior to the eruption, that continue to be active are: (1) the Tube Worm Pillar (near Biomarker #188); and (2) a spindle-shaped chimney called "Damocles Sword" present at the east margin of the ASC near Biomarker #72. A few individuals of *Riftia* and *Bathymodiolus thermophilus* were present at the base of Damocles Sword in October 1991 (Chevaldonné et al., 1995). Time-series data of vent fluid temperature for each high-temperature vent in the 9°49′N–51′N area are

presented and discussed by Oosting and Von Damm (1996). Faunal colonization patterns and development of high-temperature chimneys within the Transect are discussed in Shank et al. (in prep.).

3.2. Low-temperature vent colonization (1989–1991)

Images of the ASC floor taken using Argo in 1989 between 9°49′N and 9°51′N revealed the presence of well-developed animal communities similar to those encountered along the Galápagos Rift in 1985. Extensive beds of bathymodiolid mussels, serpulid worms, galatheid crabs, vesicomyid clams, and swarms of amphipods were observed on the margins of the ASC. The presence of only sparse populations of *Riftia pachyptila*, in a predominantly recumbent posture, and the biogeographic dominance of bathymodiolid mussels between 9°46′ and 9°52′N in 1989 suggests that these vent assemblages were in the later stages of vent community development.

During the 1991 eruption, fresh lava flows over-ran several existing communities (e.g. Tube Worm Barbecue; Fig. 1) and draped small, recently toppled chimneys (Haymon et al., 1993). At that time, high-temperature venting through bare basaltic lava and widespread unorganized diffuse flow emanating through a network of cracks, holes, deep pits, and 1–5 m wide fissures in the seafloor between 9°49.6′N and 9°50.4′N (Figs. 5a and 6a) also were observed (Haymon et al., 1993). White filamentous microbial mats, $\sim$ 1–10 cm-thick, blanketed up to 50 m^2 areas of fresh lava flows surrounding nascent venting areas. These mats were composed of a single type of bacterial "sheath-like" filament covered with particles of silica and arranged into "brittle flakes and flexible sheets" (Nelson, 1991; Haymon et al., 1993). Biogenic particles from these highly structured stratums were swept upwards from the seafloor by strong hydrothermal flow creating "snowstorms" that reached 50 m above the ASC floor (Haymon et al., 1993). In April 1991, diffuse fluid temperatures within the


Fig. 4. Video images of the principal geological features on the axial summit caldera (ASC) floor in December 1993. (a) The surface of a 1991 lava flow that ponded near the east wall (near Biomarker #110) of the ASC. The lava pillars which support the lobate crust are $\sim$ 2 m high. The extensive plates of talus in the foreground of the image are collapsed pieces of lobate crust that were once part of the flow surface. The 4–5 cm thickness of the lobate crust indicates that the 1991 flow remained ponded for $\sim$ 4 h prior to the waning of the eruption (Gregg et al., 1996). Distance across the bottom of the image is $\sim$ 4 m, and the view is to the southeast (167°). (b) The section of the axial summit caldera floor near Biomarker #175 (middle of image). Large feature in upper left is a $\sim$ 4 m tall by $\sim$ 5 m wide lava remnant created by two large lava pillars that nearly coalesced during the 1991 eruption. The "hole" in the middle served as a principal surface conduit for lateral lava movement within the axial summit caldera. The foreground is covered by platey collapse talus on a low-relief ($\sim$ 1 m) pressure ridge in the ASC floor. Distance across the bottom of the image is $\sim$ 2.5 m, and the view is to the south (173°). (c) The western margin of the primary eruptive fissure (from lower left to upper-middle of image) that fed the 1991 eruption. Clouds of "smoky" diffuse flow issue from the fissure (at left). The terrain in this video image is just south of the Bio141 and Bio142 vestimentiferan colonies (Biomarkers #143 and #144 are visible). Brachyuran and galatheid (at base of lava pillar) crabs are visible among narrow basaltic cracks lined with bacteria. The lava pillar in middle left of image is $\sim$ 4 m tall, and the view is to the south-southeast ($\sim$ 158°).
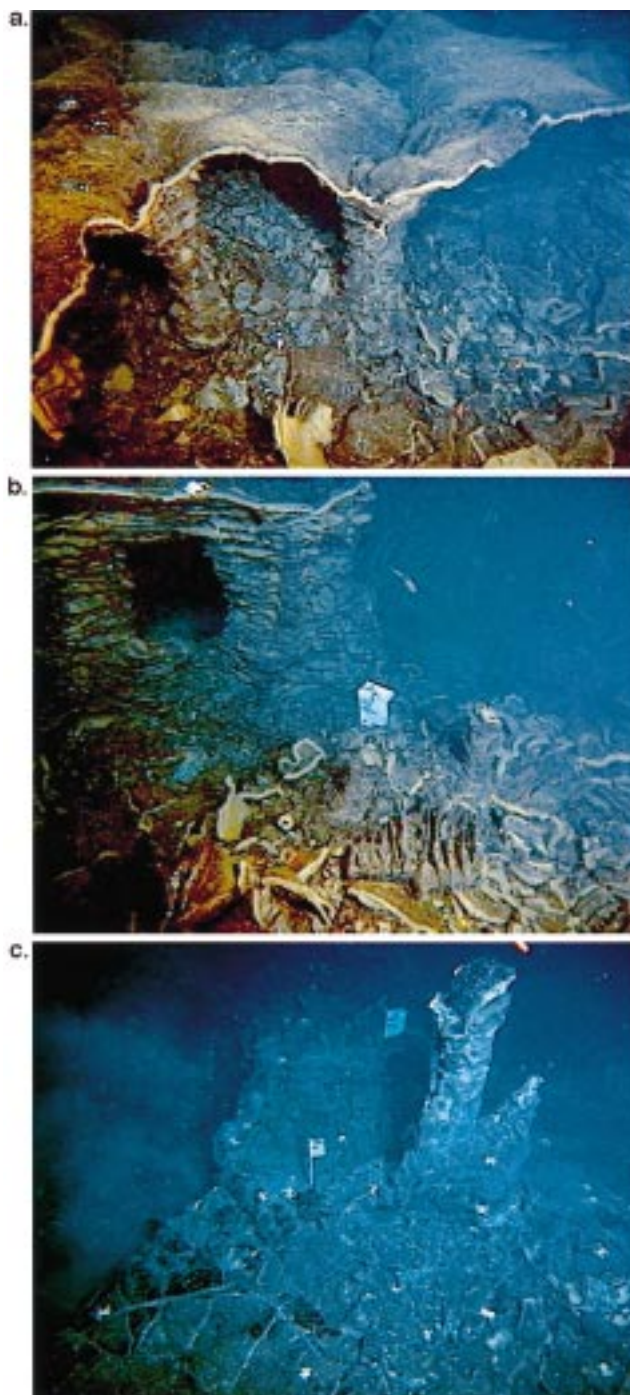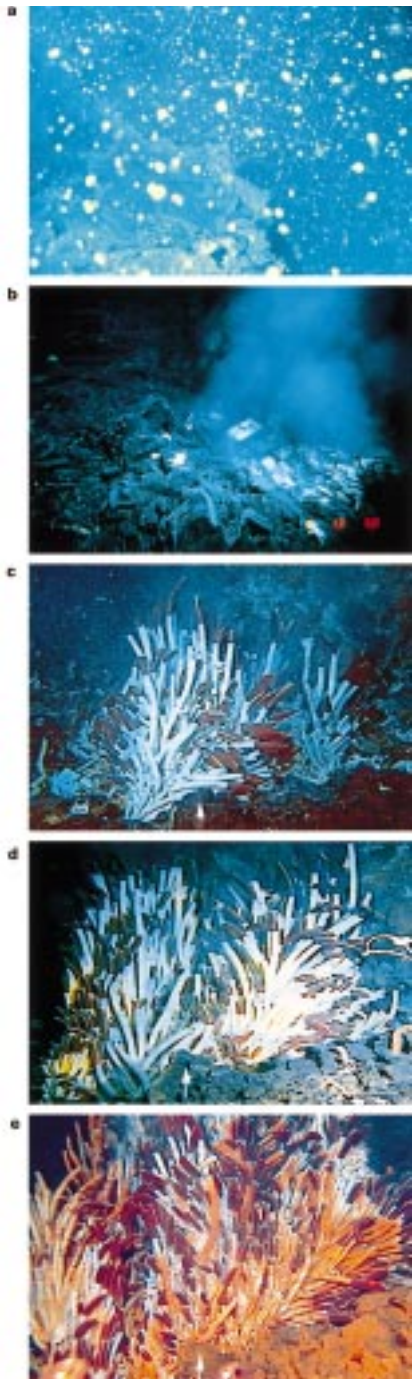
Transect ranged from 22°C (Hole-to-Hell area) to 29°C (Biomarker #141 area) to 55°C (Y Vent at the base of the Tube Worm Pillar, Fig. 1) in comparison to 2.1°C for ambient bottom water. Corresponding iron (relative to chloride) and hydrogen sulfide concentrations were unusually high (0.15 mmol kg^{-1} and 0.15–8.5 mmol kg^{-1}, respectively) in these areas. Sessile vent-endemic megafauna were not observed in any newly-formed vent openings.

3.3. Low-temperature vent colonization (1992–1995)

The sequential pattern of colonization exhibited by the dominant megafaunal species was remarkably similar within all colonies (including those spatially separated) throughout the Transect (Table 2, and Figs. 5 and 6). In every area of persistent venting, bacteria-dominated vent openings activated during the eruption were rapidly colonized and dominated by vestimentiferans; first by *Tevnia jerichonana* (within 11 months) and then by *Riftia pachyptila* (within 32 months). For convenience, these species will be referred to as *Tevnia* and *Riftia*, respectively (both are members of monospecific genera). The vent-endemic mussel *Bathymodiolus thermophilus* was initially observed adjacent (0.5–6 m distant) to these vestimentiferan colonies 10 months after the establishment of *Riftia*, and affixed to tubes of *Riftia* 13 months later. During the course of our studies we did not observe successful colonization by vesicomyid clams within the Transect area. Mullineaux et al. (1998) reports finding clams (2 ind.) identified as *Calyptogena magnifica* (of undetermined size) on basaltic settlement panels deployed near the base of P vent from December 1991 to November 1994. We observed no small specimens of clams despite intensive searching in November 1995 utilizing a macro-video camera capable of resolving 1 cm of seafloor at a camera distance of 2 m. It is conceivable, however, that vesicomyid clams occupied micro-habitats not readily discernible by macro-video (e.g. the undersurface of lobate lava crust). The observed sequence of faunal colonization (as illustrated by the Biomarker

---

Fig. 5. Temporal sequence of faunal community development at Biomarker #9 (Bio9) located along a short offset of the primary eruptive fissure in the northern Hole-to-Hell area. Arrow in c, d, and e indicates comparable corresponding location on the seafloor in successive years. (a) No vent megafaunal organisms were present when vigorous hydrothermal activity was initiated, and profuse microbial material expelled from a fissure within 15 m of the subsequent location of Biomarker #9, view is to the southeast. (b) By March 1992, the fissure was colonized by an extensive population of *Tevnia jerichonana* next to Biomarker #9, with *Riftia pachyptila* noticeably absent (view is to the northeast). (c) By December 1993, numerous *Riftia pachyptila* had settled and rapidly grown to form a dense thicket, engulfing the existing *T. jerichonana* (note Biomarker #16 at left; view is to the east, 087°). (d) Between December 1993 and October 1994, continued rapid colonization and growth by large numbers of *Riftia pachyptila* dramatically increased the density, lateral extent, and vertical growth within this colony (view is to the east, 088°). (e) By November 1995, the density and lateral extent of the Bio9 colony continued to increase. The colony was now occupied by over ~2000 *R. pachyptila*. About half of the *T. jerichonana* assemblage documented in 1992 was alive in 1995 at the base of the *R. pachyptila* tubes (*T. jerichonana* not visible in this image; view is to the east, 091°). The staining of worm tubes with a rust-colored, ferrous-oxide precipitate was coincident with increased concentrations of iron in the diffuse vent fluids (maximum temperature recorded was 33°C) supporting this colony.

#141 site, Fig. 7) and the coincident variability in vent emission and fluid chemistry are described below.

3.3.1. March 1992

Vent emissions. The reduction of widespread vent emissions between April 1991 and March 1992 formed discrete venting areas from $\sim$ 5 to 100 m^2. Thick clouds of diffuse vent flow and shimmering water exited from the primary eruptive fissure and collapsed lava pits. A marked decline in the thickness and areal extent of microbial mats reflected the spatial reduction and organization of venting over this same time period. Filamentous mats were restricted to circular patches ($\sim$1 to 10 m^2) around 17 areas of diffuse flow. Samples from several vent-associated microbial mats 300 m north of the Transect area contained extremely high abundances of siphonostomatoid copepods and pardaliscid amphipods. This high abundance prevented the accurate collection of microbial counts necessary to assess levels of microbial production (D. Nelson, pers. comm., 1993).

Megafaunal colonization. Within 11 months of the eruption, *Tevnia* colonized 17 diffuse venting areas distributed over the 900 m distance separating Biomarkers #8 and #142. These vestimentiferan-dominated areas were in discrete patches ($\sim$1 to 4 m^2) separated from each other by distances of 2 to 340 m. *Tevnia* abundance within colonies ranged from $\sim$ 30 to over 200 individuals in March 1992 (Table 2). All Transect colonies were situated on the sides of the eruptive fissures or adjacent to these fissures along numerous small cracks (coated with white microbial mats) in the ASC floor. Associated with these *Tevnia* colonies were several species of limpets (e.g. *Lepetodrilus elevatus* and *L. pustulosus*), which densely covered (100–500 ind. m^{-2}) the neighboring seafloor. These limpets were prominent within circular patches conspicuously devoid of microbial mat suggesting that these limpets were actively grazing within these mats. Brachyuran crabs (*Bythograea thermydron*) were also present on the adjacent seafloor ($\sim$ 10 ind. per colony), and were infrequently observed crawling among *Tevnia* tubes. Present on the dorsal surface of several *B. thermydron* were numerous actively "hopping" siphonostomatoid copepods (*Aphotopontius acanthinus*; Humes and Lutz, 1994). Large numbers of amphipods (*Halice hesmonectes*, Martin et al., 1993; Kaartvedt et al., 1994; Van Dover et al., 1992) swarmed $\sim$ 1 to 3 m above $\sim$ 35% (6 of 17) of the *Tevnia* colonies (Table 2).
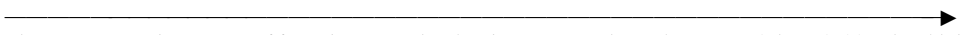
Fig. 6. Temporal sequence of faunal community development at Biomarker #119 (Bio119). (a) Microbial material and cloudy shimmering water dominated the area adjacent to the central fissure in April 1991 (view to the north, $\sim$ 007°). (b) By March 1992, a small number of *Tevnia jerichonana* were observed within this fissure (Biomarker #119 at top right; view to the south, $\sim$ 176°). (c) By December 1993, increasing numbers *T. jerichonana*, as well as several newly established *Riftia pachyptila*, were present. Zoarcid fish were also abundant (view to the north, $\sim$ 352°). (d) Between December 1993 and October 1994, *T. jerichonana* and *R. pachyptila* abundance and coverage continued to increase along the fissure, enveloping almost half of Biomarker #119 (view is to the north, 359°). (e) By November 1995, the *R. pachyptila* colony increased by $\sim$ 50 individuals, while small patches containing dead *T. jerichonana* were evident (lower right). Video image (e) was frame-captured during a spawning event by *R. pachyptila*. A spawn "cloud" is visible mid-way above the Biomarker #119 number and the top edge of the image.

9° 49' N

Legend:

- □ *Tevnia jerichonana*
- ▨ *Riftia pachyptila*
- m *Bathymodiolus thermophilus* (<20/m²)
- b *Bythograea thermydron*
- g *Munidopsis subsquamosa*
- z *Thermarces cerberus* (Zoarcidae)
- Oct octopus (n gen. n. sp.)
- ▦ serpulid polychaetes
- ⊕ amphipod swarm
- ▧ active fissure
- ■ biomarker
- — ASC wall
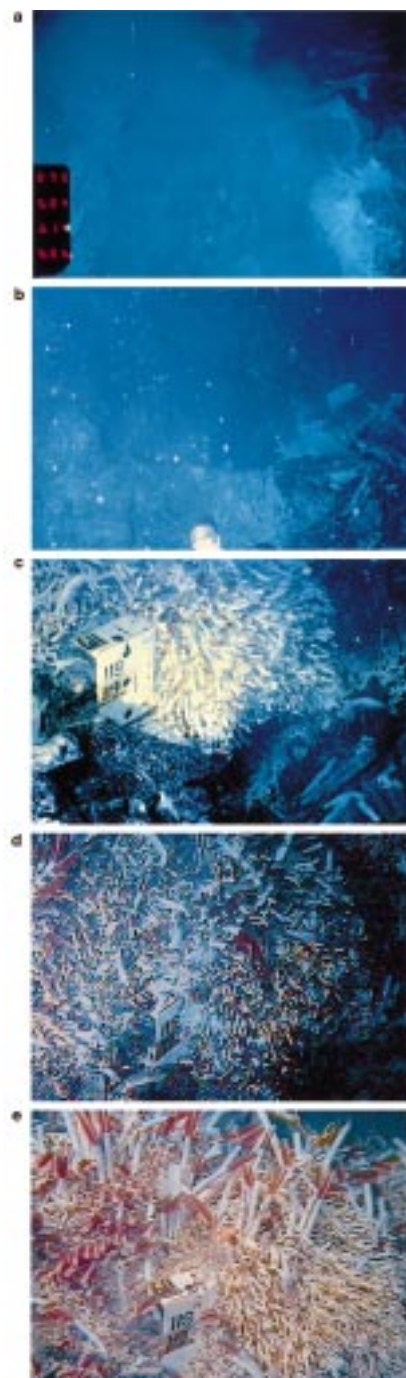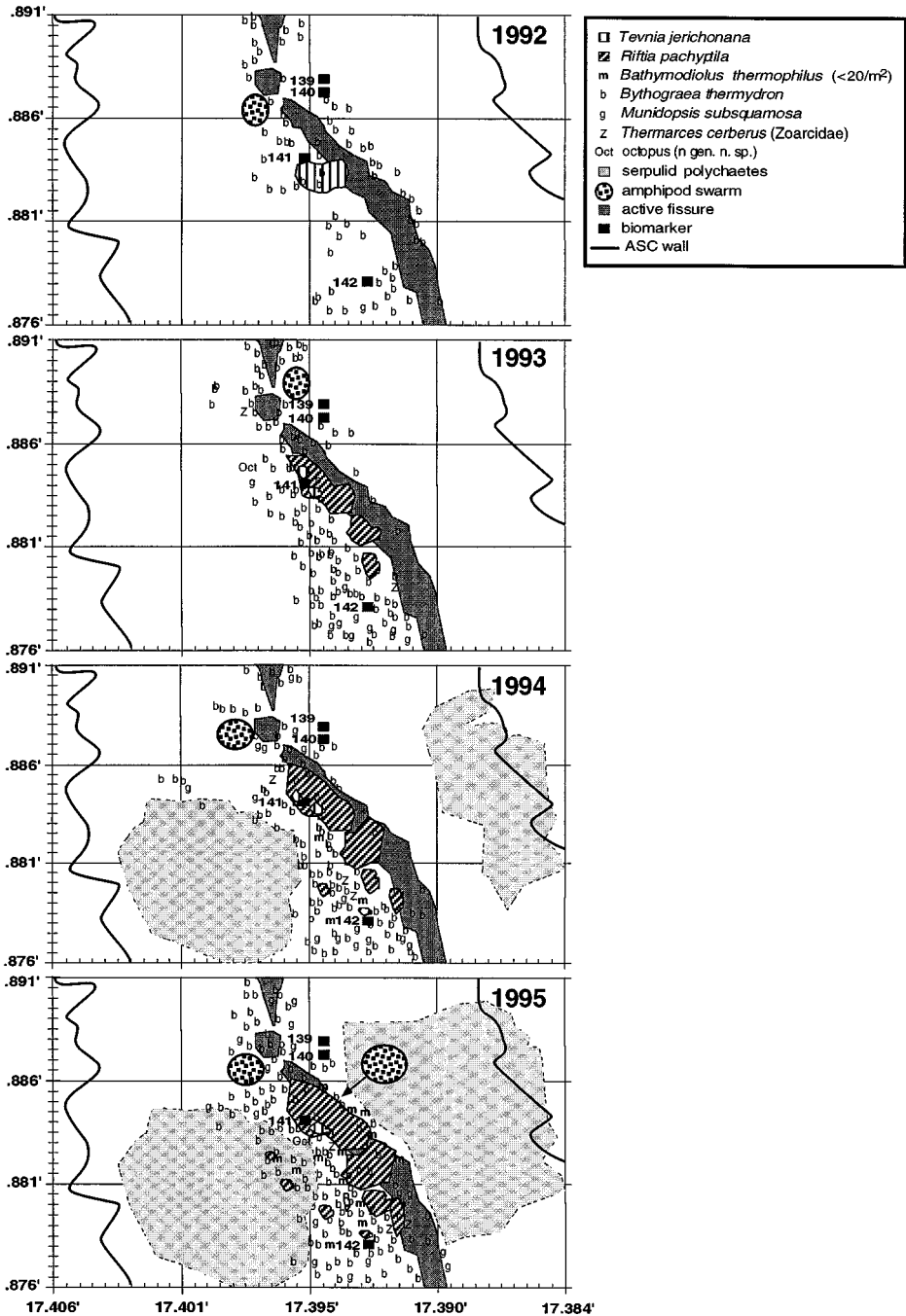
104° W

Galatheid crabs (*Munidopsis subsquamosa*) and nematocarcinid shrimp (*Nematocarcinus ensifer*?) dominated peripheral areas ($\sim$4–40 m from vent openings). The highest densities of nematocarcinids were invariably 5–20 m south of each venting area in densities (up to 0.5 m^{-2}) greater than those of galatheids.

Fluid chemistry. No low-temperature vents were sampled in March 1992, because the manifold sampler was not available for diffuse fluid sampling.

3.3.2. December 1993

Vent emissions. Spatial variability in local-scale, diffuse vent flow was evident in 1993 as venting continued to be more spatially discrete (actually ceasing in some areas) along the primary eruptive fissure. Specifically, flow was: (1) waning around the southern base of P Vent (Fig. 3); (2) completely absent between Biomarkers #40 and #81; and (3) severely reduced between Biomarkers #84 and #112. *Tevnia* and *Riftia* subjected to the cessation of vent flow were either dead (e.g. at Bio63) or dying (e.g. at Bio36 and Bio89, Table 2). Vent flow from a pit just south of P vent decreased markedly and the population of live *Tevnia* within this pit (Bio36 colony) diminished by $\sim$ 50%. This colony also contained the fewest number of *Riftia* ($\sim$ 20 ind.) within active sites along the Transect in December 1993. Unlike the slowly dying Bio36 and Bio89 colonies, rapid termination of vent flow in the Bio63 region by December 1993 coincided with the death of the Bio63 colony, and presumably preempted the successful establishment of *Riftia*. Large numbers of colonial siphonophores (*Thermopalia taraxaca*; up to 7 ind. m^{-2}) moved via their numerous long filamentous tentacles among worm tubes in these dead and dying areas (Fig. 8d). Increased densities of galatheid crabs also were associated with these moribund colonies.

Megafaunal colonization. By December 1993, 32 months after the 1991 eruption, extensive microbial mats were no longer present within the Transect. Small dense patches of microbial mat were limited to the surfaces of high-temperature chimneys. Surviving vestimentiferan colonies within the Transect region were dominated by *Riftia* (20 to over 600 ind. per colony). Linear growth rates exhibited by 1.5 m tall individuals of *Riftia* were $\sim$ 85 cm/yr (increase in tube length between March 1992 and December 1993) (e.g. Fig. 5c). These rates are the fastest reported to date for any species of vestimentiferan tube worm (Lutz et al., 1994). Extensive colonies of *Riftia* were present in each of the pre-existing *Tevnia* colonies (e.g. Bio8, Bio119 and Bio141,

---

Fig. 7. Maps depicting the temporal and spatial sequence of faunal change within the Biomarker #141 area, including the spatial distribution of Biomarkers, the aerial coverage of growing faunal assemblages, and the distribution of brachyuran and galatheid crabs in March 1992, December 1993, October 1994 and November 1995. The Biomarker #141 area features a broadening, well-defined, bacterial-stained fissure that was dominated by *Tevnia jerichonana* in 1992 and by *Riftia pachyptila* in 1993, 1994, and 1995. Mussels were first observed colonizing cracks and crevices surrounding the Bio141 colony in October 1994, and increased in abundance between October 1994 and November 1995. By November 1995, a few individual mussels were directly attached to *R. pachyptila* worm tubes. The areal coverage of serpulid polychaetes expanded over time as they encroached toward vent openings, particularly between October 1994 and November 1995. Large swarms of amphipods (*Halice hesmonectes*) were associated with vestimentiferan colonies in each year. Axis ticks = 1 m.

Table 1

Summary of the regional geological, hydrothermal, and biological characteristics of the Biologic–Geologic Transect. Marked changes in hydrothermal emissions and coincident changes in vent community structure, including the death of faunal assemblages, are featured. The ~ 17 nascent vent areas, comprising the 1.02 km-long Phoenix area, are in the northern area between Biomarkers #1 and #160. Pre-eruption communities occupy a 40 m long section on the ASC floor just north of the Southern Terminus. The Tube Worm Pillar marks the southern limit of observations made after March 1992

Transect region	Bio-marker	Distance (m)	Geological	Regional characteristics hydrothermal	Biological
Northern Terminus	1–7	40	2–7 m wide central fissure; glassy, lobate, ropy lava to sheet flow surfaces	Vigorous diffuse venting from base of fissure from Biomarker #5 south into Hole-to-Hell	Brachyuran crabs and nematocarcinid shrimp dominated fissure margin from 1992 to 1995
"Hole-to-Hell"	8–39	70	5–10 m diameter collapse pits on the margin of a 1–5 m wide fissure; ropy, hackly and sheet flow lava surfaces	High-temperature vents [Bio9 Prime and Bio9 (368°C venting from orifices in bare basalt in 1991) located in the north and P vent (368°C in 1991), P Middle, and Bucket-lid 8 vent in the south]; diffuse flow throughout the area in 1991 and 1992; by 1995, diffuse flow had increased concentrations of iron relative to hydrogen sulfide in the northern end, and diffuse vent flow had ceased in the southern end	Thick microbiol mats in 1991; in 1992, *Tevnia jerichonana* colonies near Biomarkers #8, #9, #12, #13, #29, and #36 developed along the central fissure; by 1995, vent fluids had very low H_2S and high iron concentrations within dying vestimentiferan colonies near Biomarkers #12-#13 and flow had ceased within dead colonies near Biomarkers #29-#36
South of "Hole-to-Hell"	40–99	400	2–10 m wide continuous fissure flanked by broad intermittent collapse with fresh glassy plates and broken sheet lava	Vigorous diffuse flow was associated with tube worm colonies in 1992 (29°C in 1991); by 1993, cessation of vent flow occurred north and south of Biomarker #82:; high-temperature (339°C in 1991) vent (Damaclese Sword) near Biomarker #72	*Tevnia jerichonana* colonies (Bio 61, Bio62, Bio63, Bio65, Bio66, Bio77, Bio82, and Bio89) developed by 1992. By 1993, Bio61, Bio63, Bio77, and Bio89 colonies were dead with little or no *Riftia pachyptila* colonization, while diversity and biomass increased within the Bio82 colony from 1992 to 1995
Central Transect	100–112	150	Low relief hackly and ropy lava flows with abundant collapse and lava pillar remnants	No diffuse or high-temperature venting was observed in this region	No vent-endemic megafauna were observed in this region; fauna present were nematocarcinid shrimp, synaphobranchid and macrouid fish

Biomarker #141	113–160	360	2–4 m wide central fissure bordered by sheet, hackly, and ropy lavas; fissure broadens near Biomarker #141	Intense diffuse bacterial "snowblower"-type venting (23°C) from the fissure adjacent to Biomarker #141 in 1991; fissure from Biomarker #116 to #120 and Biomarker #137 to #143 still vigorously venting diffuse flow in 1995 (27°C)	Thick microbial mats in 1991 were reduced to 1–2 m wide patches by 1992; the region between Biomarkers #117 to #121 was covered by serpulids and colonized by patches of mussels between 1994 and 1995; Bio119, Bio141, and Bio142 vestimentiferan colonies thrived from 1992 to 1995
Southern Transect	161–180	250	Highly chaotic collapse region; fissure not well-defined; numerous areas of "contact" where older sediment-dusted lobates are partially buried by younger glassy lava flows	No diffuse or high-temperature flow was observed in this region	No sessile megafauna observed in this region; area dominated by nematocarcinid shrimp and relatively few galatheid crabs
Tube Worm Pillar	181–192	40	Lobate lava fields with extensive collapse; no definable fissure in the area; mussel bed on top of lobate lava remnants on western ASC rim; an 11 m tall lava/ sulfide pillar ("Tube Worm Pillar".) is situated on a circular pedestal in a 30–40 m wide and 8–10 m deep collapse pit	No visible flow ever observed in the mussel bed; low-temperature fluid (55°C) exiting from a broken lava pillar (Y vent) at the base of the Tube Worm Pillar exhibited a high H_2S concentration, -9 mmole/kg, in 1991 which decreased to ~ 0.55 mmole/kg in 24°C fluids by 1995	Two communities existed prior to the 1991 eruption; the Biomarker #182 mussel-serpulid bed and the "Tube Worm Pillar"; mussels (no clams observed) appeared alive in 1992, but by 1995 all appeared dead; numerous galatheid crabs in the mussel bed in 1992, gastropods abundant in 1993; the Tube Worm Pillar densely inhabited by *Riftia pachyptila* since at least 1989, mobile megafauna increasing since 1991, brachyuran crabs and zoarcid fish commonly observed from 1992 to 1995
Southern Terminus	193–210	60	Series of chaotic collapse pits and lava remnants	Intense, smokey diffuse flow emanating from deep pits in 1992; spatial reduction of diffuse vent flow evident between 1992 and 1995	Brachyuran crabs were the only fauna visible due to intense water turbidity in 1992; several vestimentiferan colonies developed in this area between 1993 and 1995, but documentation is limited

Table 2

Appearance and average abundance of species, maximum diffuse fluid chemical concentrations (in mmoles kg^{-1}), and other features observed at select nascent vent areas in which vestimentiferan-dominated colonies formed within the Biologic–Geologic Transect. Colonies similar in abundance to their nearest neighboring colony are not shown here, but include Bio28, Bio59, Bio61, Bio66, Bio77, and Bio99. Observations were made within 2 weeks (April 1991), 11 months (March 1992), 32 months (December 1993), 42 months (October 1994) and 55 months (November 1995) from the initiation of venting activity. Abundance estimates include $\sim 1\ m^2$ of seafloor surrounding each colony ($*$ = vestimentiferan colony on fissure margin only; † = sample taken in the vicinity; ‡ = limit of detection; — = not observed (despite detection efforts) or sampled; ( ) = empty tubes, animals considered dead; ND = temperature anomaly not detected)

Species/Feature	Transect Colony									
	Bio8					Bio9				
	91	92	93	94	95	91	92	93	94	95
Bacterial mats	$> 20\ m^2$	$< 5\ m^2$	—	—	—	$> 20\ m^2$	$< 5\ m^2$	—	—	—
Bythograea thermydron	10	10	10	20	30	—	10	10	10	20
Thermarces andersoni	1	1	< 5	< 5	< 10	—	< 5	< 5	< 5	< 5
Lepetodrilus spp.	—	100	150	200	> 300	—	100	200	350	> 400
Tevnia jerichonana	—	200	100	50	50	—	150	100	50	50
Riftia pachyptia	—	—	600	1100	2000	—	—	400	800	2000
Amphipod spp.	—	—	—	30	50	—	—	30	30	90
Alvinocaris lusca	—	—	—	—	—	—	—	< 5	< 5	< 5
Paralvinella grasslei	—	—	—	—	—	—	—	—	—	—
Thermopalia taraxaca	—	—	—	—	—	—	—	—	—	—
Munidopsis subsquamosa	—	—	—	—	1	—	—	—	—	—
Halice hesmonectes swarm	—	—	—	—	—	—	—	—	—	—
Bathymodiolus thermophilus	—	—	—	< 5	< 15	—	—	—	—	—
Serpulid polychaetes (per m^2)	—	—	—	—	—	—	—	—	—	—
Cyanathea hydrothermala	—	—	—	—	2	—	—	—	—	—
R. pachyptila spawning event	—	—	—	—	—	—	—	—	—	—
Temperature (max. °C)	—	—	—	—	—	22†	—	—	32	33
Methane	—	—	—	—	—	—	—	—	0.004	0.005
Carbon dioxide	—	—	—	—	—	—	—	—	8.4	8.8
Iron	—	—	—	—	—	—	—	—	0.064	0.240
Hydrogen sulfide	—	—	—	—	—	—	—	—	0.80	0.194

Table 2. Continued

Species/Feature	Transect Colony									
	Bio12					Bio13				
	91	92	93	94	95	91	92	93	94	95
Bacterial mats	> 20 m²	< 5 m²	—	—	—	> 20 m²	< 5 m²	—	—	—
Bythograea thermydron	—	10	10	10	5	—	10	10	10	10
Thermarces andersoni	—	< 5	< 5	< 5	< 5	—	5	5	5	5
Lepetodrilus spp.	—	100	200	200	< 40	—	200	200	200	—
Tevnia jerichonana	—	30	30	30	(30)	—	50	50	50	(50)
Riftia pachyptila	—	—	200	250	10(250)	—	—	200	200	25(200)
Amphipod spp.	—	—	20	20	10	—	—	—	—	—
Alvinocaris lusca	—	—	—	—	—	—	—	—	—	—
Paralvinella grasslei	—	—	—	—	—	—	—	—	—	—
Thermopalia taraxaca	—	—	—	—	—	—	—	—	—	—
Munidopsis subsquamosa	—	—	—	1	3	—	—	—	—	—
Halice hesmonectes swarm	—	—	1	1	—	—	1	—	—	—
Bathymodiolus thermophilus	—	—	—	< 5	—	—	—	—	< 5	—
Serpulid polychaetes (per m²)	—	—	—	—	—	—	—	—	—	—
Cyanathea hydrothermala	—	—	—	—	—	—	—	—	—	—
R. pachyptila spawning event	—	—	—	—	—	—	—	—	—	—
Temperature (max. °C)	—	—	—	—	29	—	—	—	—	—
Methane	—	—	—	—	0.0003	—	—	—	—	—
Carbon dioxide	—	—	—	—	5.2	—	—	—	—	—
Iron	—	—	—	—	0.28	—	—	—	—	—
Hydrogen sulfide	—	—	—	—	⩽ 0.015[‡]	—	—	—	—	—

Table 2. Continued

Species/Feature	Transect Colony									
	Bio36					Bio63				
	91	92	93	94	95	91	92	93	94	95
Bacterial mats	> 20 m²	> 5 m²	—	—	—	> 20 m²	> 5 m²	—	—	—
Bythograea thermydron	—	10	10	10	10	—	10	—	—	—
Thermarces andersoni	1	—	—	5	5	—	—	—	—	—
Lepetodrilus spp.	—	—	—	—	—	—	> 500	—	—	—
Tevnia jerichonana	—	150	100(100)	(150)	(150)	—	150	(200)	(200)	(200)
Riftia pachyptila	—	—	20	(20)	(20)	—	—	—	—	—
Amphipod spp.	—	—	—	—	—	—	—	—	—	—
Alvinocaris lusca	—	—	< 5	< 5	< 5	—	—	—	—	—
Paralvinella grasslei	—	—	—	—	—	—	—	—	—	—
Thermopalia taraxaca	—	—	—	—	—	—	—	< 20	—	—
Munidopsis subsquamosa	—	—	—	< 5	< 5	—	—	< 5	< 5	—
Halice hesmonectes swarm	—	1	—	—	—	—	—	—	—	—
Bathymodiolus thermophilus	—	—	—	—	—	—	—	—	—	—
Serpulid polychaetes (per m²)	—	—	—	—	—	—	—	—	—	—
Cyanathea hydrothermala	—	—	—	—	—	—	—	—	—	—
R. pachyptila spawning event	—	—	—	—	—	—	—	—	—	—
Temperature (max. °C)	—	—	—	—	—	—	—	—	ND	9
Methane	—	—	—	—	—	—	—	—	—	—
Carbon dioxide	—	—	—	—	—	—	—	—	—	—
Iron	—	—	—	—	—	—	—	—	—	—
Hydrogen sulfide	—	—	—	—	—	—	—	—	—	—

Table 2. Continued

Species/Feature	Transect Colony									
	Bio82					Bio89				
	91	92	93	94	95	91	92	93	94	95
Bacterial mats	> 20 m^2	> 5 m^2	—	—	—	> 20 m^2	> 5 m^2	—	—	—
Bythograea thermydron	—	10	10	20	30	—	10	20	10	10
Thermarces andersoni	—	—	5	10	15	—	—	5	5	5
Lepetodrilus spp.	—	> 200	> 400	> 600	> 2000	—	> 500	200	—	—
Tevnia jerichonana	—	200	200	200(50)	250(50)	—	150	500(500)	(1000)	(1000)
Riftia pachyptila	—	—	600	800	> 2000	—	—	200	(200)	(200)
Amphipod spp.	—	—	30	30	50	—	—	—	—	—
Alvinocaris lusca	—	—	—	—	< 10	—	—	—	—	—
Paralvinella grasslei	—	—	—	—	—	—	—	—	—	—
Thermopalia taraxaca	—	—	—	—	—	—	—	< 5	—	—
Munidopsis subsquamosa	—	—	—	—	—	—	—	—	< 5	< 5
Halice hesmonectes swarm	—	1	1	1	1	—	—	—	—	—
Bathymodiolus thermophilus	—	—	—	10	50	—	—	—	—	—
Serpulid polychaetes (per m^2)	—	—	—	—	—	—	—	—	—	—
Cyanathea hydrothermala	—	—	—	—	—	—	—	—	—	—
R. pachyptila spawning event	—	—	1	1	1	—	—	—	—	—
Temperature (max. °C)	29[†]	—	16	20	18	—	—	—	ND	ND
Methane	—	—	0.002	0.003	0.002	—	—	—	—	—
Carbon dioxide	—	—	5.6	6.2	5.8	—	—	—	—	—
Iron	—	—	0.024	0.003	0.011	—	—	—	—	—
Hydrogen sulfide	1.01[†]	—	—	0.4	0.263	—	—	—	—	—

Table 2. Continued

Species/Feature	Transect Colony									
	Bio119					Bio141*				
	91	92	93	94	95	91	92	93	94	95
Bacterial mats	> 20 m²	> 5 m²	—	—	—	> 20 m²	> 5 m²	—	—	—
Bythograea thermydron	—	10	10	50	150	—	10	10	20	30
Thermarces andersoni	—	5	15	10	15	—	—	10	30	35
Lepetodrilus spp.	—	> 200	> 2000	> 2000	> 2000	—	> 200	> 400	> 600	> 2000
Tevnia jerichonana	—	50	150	500	1000(250)	—	100	200	250	250
Riftia pachyptila	—	—	50	150	200(25)	—	—	400	800	> 2000
Amphipod spp.	—	—	30	30	50	—	—	30	35	60
Alvinocaris lusca	—	—	—	—	< 5	—	—	—	—	—
Paralvinella grasslei	—	—	—	—	—	—	—	> 20	> 20	> 20
Thermopalia taraxaca == ==	== — ==	== — ==	== — ==	== — ==	== — ==	== — ==	== — ==	== — ==	== — ==	== — ==
Munidopsis subsquamosa	—	—	—	—	—	—	—	—	—	—
Halice hesmonectes swarm	—	1	1	1	1	—	1	1	1	1 +
Bathymodiolus thermophilus	—	—	—	5	< 30	—	—	—	< 10	< 15
Serpulid polychaetes (per m²)	—	—	—	—	< 50	—	—	—	—	< 50
Cyanathea hydrothermala	—	—	—	—	—	—	—	—	—	—
R. pachyptila spawning event	—	—	—	—	1	—	—	2	1	1
Temperature (max. °C)	—	—	—	—	—	23[†]	—	26	29	27
Methane	—	—	—	—	—	—	—	0.002	0.009	0.008
Carbon dioxide	—	—	—	—	—	—	—	9.4	6.7	8.7
Iron	—	—	—	—	—	0.004[†]	—	0.021	0.012	0.012
Hydrogen sulfide	—	—	—	—	—	1.9[†]	—	0.944	0.88	0.725

Table 2. Continued

Species/Feature	Transect Colony				
	Bio142				
	91	92	93	94	95
Bacterial mats	> 20 m²	> 5 m²	—	—	—
Bythograea thermydron	—	10	10	10	10
Thermarces andersoni	—	—	10	35	25
Lepetodrilus spp.	—	—	> 200	> 400	> 400
Tevnia jerichonana	—	50	50	50	50
Riftia pachyptila	—	—	400	600	800
Amphipod spp.	—	—	—	—	—
Alvinocaris lusca	—	—	—	—	—
Paralvinella grasslei	—	—	> 20	> 20	> 20
Thermopalia taraxaca	—	—	—	—	—
Munidopsis subsquamosa	—	—	—	—	1
Halice hesmonectes swarm	—	—	—	1	1 +
Bathymodiolus thermophilus	—	—	—	< 15	< 75
Serpulid polychaetes per m²)	—	—	—	—	< 10
Cyanathea hydrothermala	—	—	—	—	—
R. pachyptila spawning event	—	—	1	—	1
Temperature (max. °C)	—	—	35	28	18
Methane	—	—	0.030	0.004	0.002
Carbon dioxide	—	—	11.6	2.7	4.8
Iron	—	—	0.028	0.005	0.012
Hydrogen sulfide	—	—	0.979	0.68	0.301

Figs. 5 and 6). Individuals of *Riftia* reached maturity in less than 20 months as evidenced by the documentation of four separate spawning events (a rapid ejection of a cloudy material released from a single point below the obturaculum) within three distinct colonies during 12 dives in December 1993 (Table 2).

The characteristic "haystack" morphology where *Riftia* tubes centrally located within a colony were at least twice as tall as those inhabiting the periphery [described by Hessler and Smithey (1983) and Hessler et al. (1985, 1988)], was displayed by *Riftia* assemblages containing more than nine individuals. The length of these *Riftia* tubes was proportional to the visually estimated intensity of vent emissions, suggesting that *Riftia* growth was optimized for proximal venting conditions. Individuals of *Riftia* did not appear to be limited to areas previously colonized by *Tevnia* populations. Seemingly sporadic, opportunistic colonization by *Riftia* was apparent as tufts comprised of 2–35 individuals, frequently colonized lava pillars, cracks, and areas between lobate lava surfaces from which shimmering vent fluids emanated.

Faunal diversity, as determined from video analyses, increased from at least 5 species [bythograeid crabs, lepetodrilid limpets (perhaps 3 species), siphonostomatoid copepods, zoarcid fish, tevniid tube worms] in March 1992, to at least 11 species (additionally, bresiliid shrimp, alvinellid polychaetes, nebaliid leptostracans, pardaliscid and lysianassid amphipods, and riftiid tube worms) in December 1993 (Table 2). In December 1993, the bresiliid shrimp *Alvinocaris lusca* was observed among tubes of *Riftia* only at the extreme northern (Bio9, 5 ind.) and southern ends (Tube Worm Pillar, 2 ind.) of the Transect. The polychaetous annelid *Paralvinella grasslei* (present at the base of *Riftia* tubes, Fig. 8a) was seen in only the Bio141 and Bio142 colonies, and never observed in any other *Riftia* colonies in the Transect area.

Fluid chemistry. Maximum diffuse fluid temperatures within the central and southern colonies varied from 16°C to 35°C in December 1993. Maximum hydrogen sulfide concentrations declined from 1.9 mmol kg^{-1} in April 1991 to 0.979 mmol kg^{-1} in December 1993 (Table 2). Maximum diffuse fluid iron concentrations within vestimentiferan colonies declined more sharply from 0.151 mmol kg^{-1} in April 1991 to 0.024 mmol kg^{-1} in December 1993. Within these same colonies, methane concentrations varied from 0.002 to 0.030 mmol kg^{-1} and carbon dioxide concentrations ranged from 5.6 to 11.6 mmol kg^{-1} (Table 2).

---→

Fig. 8. Continued

individuals in this image are less than $\sim$ 20 cm in length). (d) By December 1993, venting emissions had completely ceased in the Bio63 colony and no living vestimentiferans (less than 5 *Riftia pachyptila* had colonized this area) were observed (view is to the southwest, 192°; distance across the bottom edge of image is $\sim$ 3 m). The only living megafaunal organisms among the worm tubes were numerous rhodalid siphonophores (*Thermopalia taraxaca*). *T. taraxaca* moved amongst the worm tubes and over the adjacent basalt via their long filamentous tentacles. (e) In December 1993 and October 1994 the Bio12 colony was a *Riftia pachyptila* assemblage (with associated dense amphipods) typical of those within the Transect at these times. However by November 1995 (shown here), the entire colony and much of the surrounding seafloor was covered with a rust-colored iron-oxide precipitate, and over 95% of the *R. pachyptila* were dead, despite the extensive schlieren of 29°C fluids throughout the moribund colony. (f) Amphipod swarms reached up to 18 m^3 above *R. pachyptila* colonies as shown here above the Bio141 colony in November 1995.
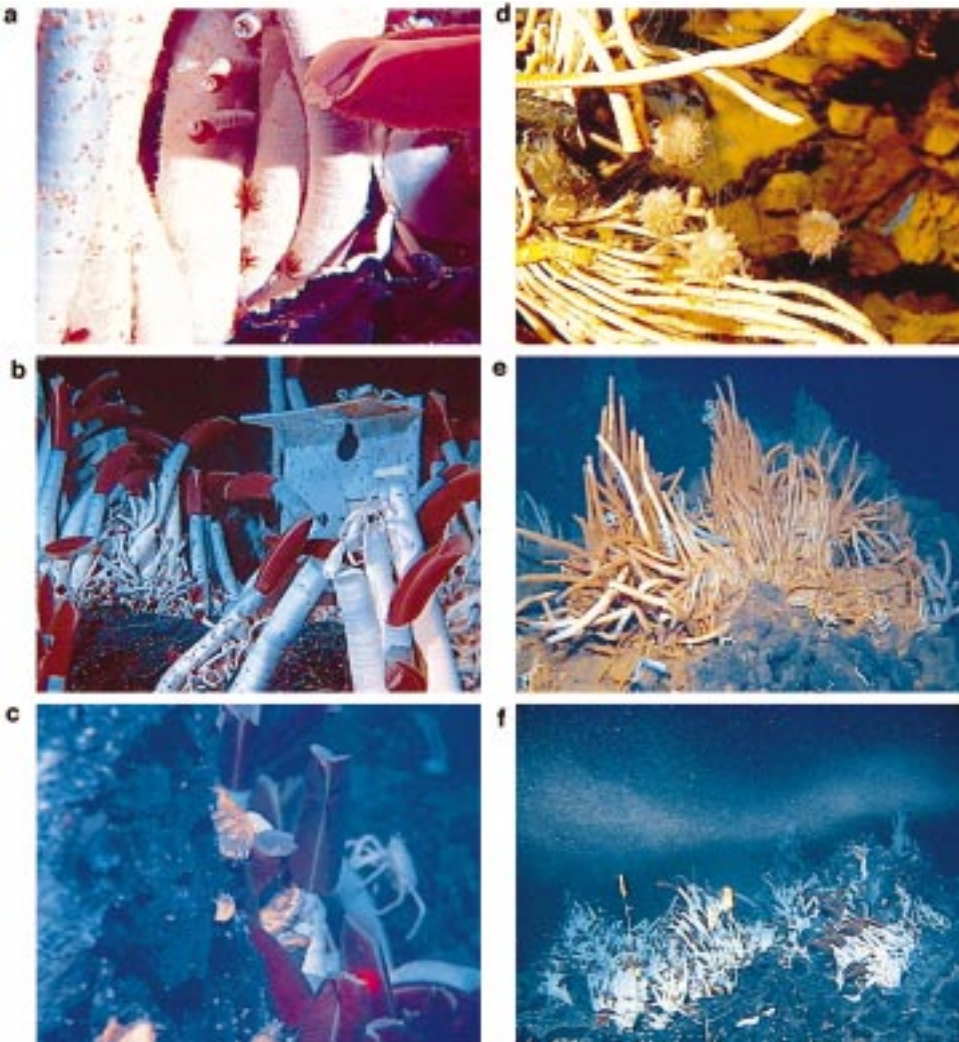
Fig. 8. Video images illustrating characteristics of community structure within developing and dying colonies and their associated abiotic habitat. (a) *Paralvinella grasslei* was observed between the basal portion of *Riftia pachyptila* tubes within the Bio141 colony (four individuals shown here; view is toward the east in 1993; distance across the lower edge of the image is ∼ 25 cm; note small *R. pachyptila* at lower left and the presence of highly variable lepetodrilid limpet abundance on certain worm tubes). This was the only vestimentiferan colony in which *P. grasslei* was observed. (b) Within several vestientiferan colonies, *Tevnia jerichonana* displayed gregarious settlement and colonization as indicated by numerous small individuals observed here (arrow) in December 1993 near Biomarker #141 (view is to the northeast). (c) The first documented occurrence of a glalatheid crab directly on the surface of a *Riftia pachyptila* tube (at right) took place in November 1995, 55 months after the April 1991 eruption. Mussel (*Bathymodiolus thermophilus*) densities observed in this image were typical of the densities observed adjacent to the Bio142 colony in November 1995 (note byssal threads on yellow-brown mussel shells; view is to the southeast; *T. jerichonana*

3.3.3. October 1994

Venting emissions. The only evident variation in vent flux between December 1993 and October 1994 was the cessation of diffuse flow in areas already waning in December 1993 (e.g. near P vent, Biomarker #84 and #112). All *Tevnia* and *Riftia* living proximal to these areas were dead by October 1994 (e.g. Bio89, Table 2). Microbial mats were no longer observed within the Transect area. However, hyperthermophilic methanotrophic bacteria were isolated from diffuse fluids within the Bio9 *Riftia* colony as well as from the base of the Tube Worm Pillar.

Megafaunal colonization. Between December 1993 and October 1994, individuals of *Riftia* within thriving colonies grew an additional 0.2–1.0 m. The number of *Riftia* continued to increase, doubling their densities in certain colonies (e.g. Bio8 and Bio9). The amount of seafloor area occupied by *Riftia* increased little ($<1 \, \text{m}^2$) in the northern colonies, while central (Bio82 and Bio119) and southern colonies (Bio141 and Bio142) expanded along the primary fissure by an additional ~ 2–$10 \, \text{m}^2$, suggesting that the carrying capacity of *Riftia* in these areas had not been reached in December 1993. Between December 1993 and October 1994, *Tevnia* (with their tightly aggregated tubes forming small tufts; Fig. 8b) continued to colonize the *Riftia*-dominated colonies. Individuals of *Tevnia* identified as alive in December 1993 were still alive in October 1994. By October 1994, small bathymodiolid mussels (~ 2–$11 \, \text{cm}$ long) were nestled under pieces of basaltic talus and in narrow cracks in the seafloor within 0.5–6 m of the tube worm assemblages (Fig. 8c, Table 2). Within adjacent ($1 \, \text{m}^2$) areas of seafloor surrounding the Transect colonies, mussel densities averaged 1–$3 \, \text{m}^{-2}$, with an average of 9 individuals around a given *Riftia* community (Table 2). The greatest mussel density ($5 \, \text{m}^{-2}$) was observed near the Bio141 and Bio142 colonies.

Fluid chemistry. Concomitant with the observed faunal changes between December 1993 and October 1994 was a continued decline of hydrogen sulfide and iron concentrations in $20°$–$32°\text{C}$ diffuse fluids (Table 2). In October 1994, hydrogen sulfide concentrations ranged from $0.40 \, \text{mmol kg}^{-1}$ in the central (Bio82) Transect region to $0.68 \, \text{mmol kg}^{-1}$ ($\sim 0.3 \, \text{mmol kg}^{-1}$ lower than in December 1993) in the southern (Bio141 and Bio142) region and $0.80 \, \text{mmol kg}^{-1}$ in the northern Hole-to-Hell area (Bio9). Colonies that exhibited the largest increase in tube worm abundance between December 1993 and October 1994 (e.g. Bio9 and Bio141) also contained the highest H_2S concentrations. Maximum methane concentrations decreased from $0.03 \, \text{mmol kg}^{-1}$ in December 1993 to $0.009 \, \text{mmol kg}^{-1}$ in October 1994 (varied from 0.003 to 0.009). Carbon dioxide concentrations decreased dramatically from 9.4 and $11.6 \, \text{mmol kg}^{-1}$ to 6.7 and $2.7 \, \text{mmol kg}^{-1}$ within the southern Bio141 and Bio142 colonies, respectively, while carbon dioxide concentrations increased slightly from 5.6 to $6.2 \, \text{mmol kg}^{-1}$ within the central Transect's Bio82 colony (Table 2).

3.3.4. November 1995

Vent emissions. In November 1995, no spatial displacement of vent emissions was detected and no additional cessation of flow was observed since the previous visit in October 1994. However, vent openings that supported the Bio63 colony in March 1992 and ceased venting by December 1993 had been reactivated between October

1994 and November 1995 with 9°C vent fluids. No faunal response to this reactivation was evident. Worm tubes of *Tevnia* (dead since December 1993) in this colony showed little decay or weathering after 23 months. Vent emissions in the central transect area not only increased in intensity, but the areal extent of the Bio82 and Bio119 colonies increased up to 20 m^2 more than the northern and southern colonies, where the average areal increase was 3 m^2.

Megafaunal colonization. Tevnia continued to colonize in tufts (~ 20 ind. per colony) within *Riftia* communities. A few groups of *Tevnia* observed alive in December 1993 were also identified as being alive in November 1995. The number of dead *Tevnia* observed within *Riftia* colonies also increased between October 1994 and November 1995 (e.g. at Bio119, Table 2), despite persistent vent flow. In November 1995, dead *Tevnia* (tufts of empty tubes) were present in all active colonies except Bio141 and Bio142. *Riftia* colonization dramatically increased at all active vents within the Transect area (e.g. Bio9, Bio82, Bio141, and Y vent at the base of Tube Worm Pillar). The increasingly dense matrix of vestimentiferan tubes (since 1993) provided micro-habitats for expanding numbers of amphipods, leptostracans, and limpets (Table 2).

By November 1995 (55 months after the initiation of venting), *Bathymodiolus thermophilus* colonized the seafloor surrounding every surviving vestimentiferan colony in the Transect except the one at Bio9 (Table 2). Mussels (less than 12 ind., 3–10 cm in length) were observed to be attached to tubes of *Riftia* (Fig. 8d), but only in the southernmost colonies (Bio141 and Bio142). Mussel colonization surrounding the central Bio119 colony was the most extensive along the Transect, as mussels formed tight clumps (4–12 ind.) and linear rows within cracks that were spread over a 120 m^2 area. The largest mussel (12 cm) within the Transect was observed in this area. The abundance of serpulid polychaetes (*Laminatubus alvini* and *Protis hydrothermica*, indistinguishable in video) was extremely high (up to 125 ind. m^{-2}) from the location of the Bio119 colony in the central fissure across the low-relief ASC floor up to and on top of the adjacent ASC walls. Serpulids also encroached in greater numbers from peripheral areas around the Bio141 and Bio142 colonies to within centimeters of the base of *Riftia* tubes. Abundances of both mussels and serpulids were much lower in the northern end (Hole-to-Hell area) of the Transect. The first appearance of anemones (3 ind. of *Cyanathea hydrothermala*, based on descriptions in Doumenc and Van-Praët, 1988) within the Transect area was observed in November 1995 on slightly iron-stained basaltic talus adjacent to the Bio8 colony.

The biological and geochemical changes that occurred within the Bio12 colony in the northern Hole-to-Hell area were in marked dissimilarity to the range of biological and geochemical changes that took place within the rest of the Transect colonies between October 1994 and November 1995. The 29°C vent fluids bathing the Bio12 colony in November 1995 contained extremely low concentrations of H$_2$S (at the limit of detection: 0.015 mmol kg^{-1}) and relatively high concentrations of iron (~ 0.28 mmol kg^{-1}, Table 2). Methane concentrations of 0.0003 mmol kg^{-1} in the Bio12 fluids were an order of magnitude lower than previously observed within the Transect, while concentrations of carbon dioxide (5.2 mmol kg^{-1}) were similar to those in other Transect colonies. Rust-colored ferrous-oxide precipitation coated the entire vestimentiferan colony, including brachyuran crabs, limpets, as well as much of the surrounding seafloor

(partially staining the Bio9 colony 4 m to the north, Fig. 5e). Only 10 of the ~ 250 individuals of *Riftia* comprising this colony were considered to be alive (plumes observed). No *Thermopalia taraxaca* ("dandelions"), commonly observed among dead colonies lacking vent flow in December 1993, were observed within this dying assemblage.

Fluid chemistry. Between October 1994 and November 1995, H_2S concentrations within diffuse fluids continued to decline in the Bio9, Bio82, and Bio142 colonies (from 0.40–0.80 mmol kg^{-1} to 0.194–0.301 mmol kg^{-1}) with a slight increase only in the Bio141 colony (from 0.68 to 0.725 mmol kg^{-1}) (Table 2). Maximum diffuse fluid temperatures in the Transect colonies declined by as much as 10°C. Methane concentrations showed only a slight general decrease between October 1994 and November 1995 (Table 2). Maximum measured iron concentrations remained low in the central and southern colonies (~ 0.011 mmole kg^{-1} in Bio82 and 0.012 mmole kg^{-1} in Bio141 and Bio142).

3.4. Patterns of mobile fauna distribution ("Transect Runs")

In April 1991, only six brachyuran crabs (*Bythograea thermydron*) and one zoarcid fish (*Thermarces cerberus*) were documented along the length of the Transect. During the next 11 months, the abundance of mobile vent organisms [e.g. *Aphotopontius acanthinus*, *Halice hesmonectes*, *Bythograea thermydron*, *Cyanograea predaetor*, *Munidopsis subsquamosa*, *Thermarces cerberus*, and an octopus (n. gen. n. sp., E. Hochberg, pers. comm., 1996)] and mobile "non-vent" organisms (principally nematocarcinid shrimp) dramatically increased within the Transect. Over 1207 brachyuran crabs, 127 galatheid crabs, 91 nematocarcinid shrimp, 17 zoarcid fish, 12 amphipod swarms, and 6 octopods were observed during a north to south transect survey in March 1992. During transect runs between March 1992 and November 1995, the abundance of brachyuran and galatheid crabs increased by $\sim 12\%$ and 137%, respectively; nematocarcinids increased by $\sim 8\%$, and zoarcids by a marked 892%. Dense "swarms" of a new species of pardaliscid amphipod, *Halice hesmonectes* (Martin et al., 1993), were observed maintaining their position within meters above low-temperature diffuse venting and shimmering water (Kaartvedt et al., 1994; Van Dover et al., 1992). These "swarms" are believed to represent the greatest density of invertebrates known in the deep sea, as numbers have been reported in excess of 1000 individuals per liter (Van Dover et al., 1992). Previous measurements of volume occupied by these swarms was < 1 m^3 (Kaartvedt et al., 1994), while our observations indicate that these swarms can occupy an area as small as ~ 1 m^3 above small groups of mussels and up to ~ 18 m^3 overlying *Riftia* assemblages (Fig. 8f). The distribution and abundance of amphipod swarms and octopods (1 ind. sighted within ~ 10 m of same location each year suggesting territoriality) remained remarkably constant in successive years. Amphipod swarms were observed above the same active vestimentiferan colonies (e.g. Bio12, Bio82, Bio119, and Bio141) from year to year (Table 2).

Changes in the distribution of brachyuran and galatheid crabs between March 1992 and November 1995 reflected the redistribution and cessation of venting emissions over this time period (Fig. 9). Both species increased in density closer to the vent openings, and galatheids (and nematocarcinid shrimp) tended to increase in density

just south of active vestimentiferan colonies. Both species of crabs were evenly distributed along the Transect in March 1992, when diffuse flow was vigorous, unorganized, and not yet as spatially discrete as in December 1993. As flow became focused over time, the density of both crab species increased near diffuse and high-temperature venting areas within the Transect (Fig. 9). The relative changes in galatheid distribution paralleled those of brachyurans until November 1995, when the number of galatheids increased from ~50 to over 264 individuals between Bio-markers #114 and #120 resulting in higher densities than brachyurans (Fig. 9). This shift in galatheid distribution was coincident with the most pronounced and widespread colonization of mussels and serpulids (near the Bio119 colony) in the Transect. At other sites in the eastern Pacific (e.g. 13°N EPR and Galápagos Rift), galatheid crabs are commonly observed walking among vestimentiferan tubes. However, galatheid crabs were never observed among or within a meter of any of the newly-established vestimentiferan colonies within the Transect until 55 months after the eruption (and then only one individual within the Bio8 and Bio142 colonies) (Fig. 8c).

4. Discussion

4.1. Rates of biological processes on the fast-spreading East Pacific Rise

Since the discovery of deep-sea hydrothermal vents in 1976, there has been a growing body of evidence that rates of certain biological processes proceed relatively rapidly in these unusual environments (Grassle, 1985; Lutz et al., 1988; Roux et al., 1989; Tunnicliffe, 1991; Childress and Fisher, 1992). Documented temporal and spatial changes within the Transect area provide dramatic, unambiguous evidence that rates of colonization and growth of vestimentiferan tube worms, as well as diverse faunal assemblages, are extremely rapid at deep-sea hydrothermal vents. The fastest rates of growth reported for both *Tevnia* (~30 cm/yr) and *Riftia* (~85 cm/yr) were exhibited in the northern Hole-to-Hell area (Lutz et al., 1994). The rapid establishment of 17 *Tevnia* colonies in virtually every locale where diffuse sulfide-rich hydrothermal discharge was most intense in April 1991 suggests that *Tevnia* is a more effective colonizer than other megafaunal species associated with these fast-spreading MOR systems. Abundance estimates obtained 11 months after the eruption, from colonies spanning 1 km of seafloor, suggest that founding population size of *Tevnia* on fast-spreading MORs may average between ~30–150 ind. per colony. The presence of *Tevnia* with highly variable tube lengths (up to 30 cm) within each of the colonies suggests the possibility of either continuous recruitment or a single recruitment event containing individuals with highly variable, environmentally driven, growth rates. Observations within the Transect also indicate that adult *Tevnia* are more tolerant of higher temperatures and sulfide concentrations than *Riftia*, as individuals preferentially colonized the most vigorous H_2S-rich diffuse venting areas, and active chimney surfaces. The presence of numerous dead *Tevnia* (that were documented alive in previous years) coexisting with live *Riftia* and *Tevnia* suggests that, under conditions
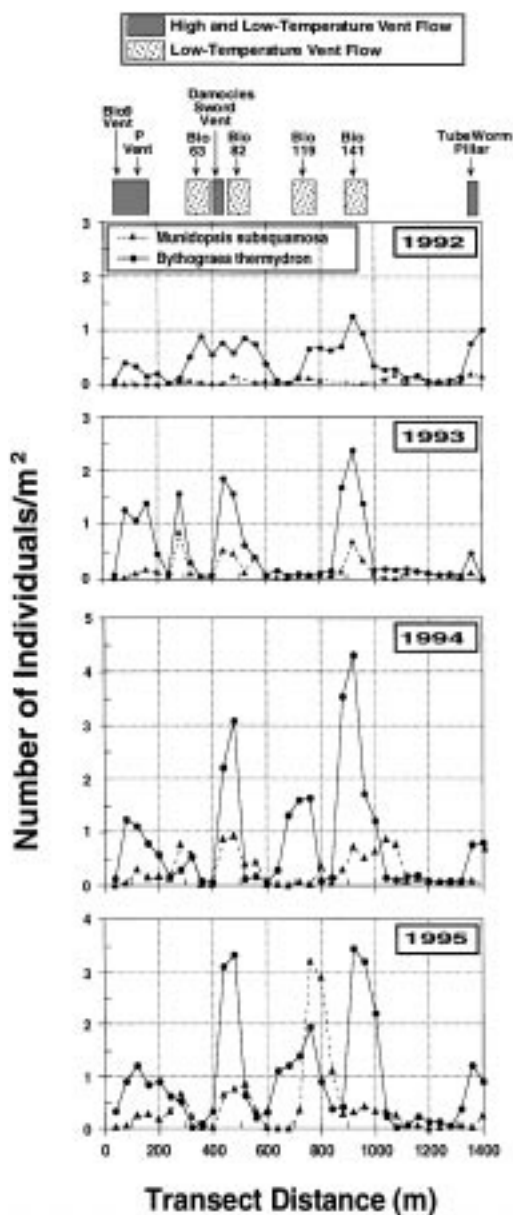
Fig. 9. The temporal distribution and density of brachyuran and galatheid crabs along the Transect between March 1992 and November 1995. Nematocarcinid shrimp densities (not shown here) closely mirrored those of galatheid crabs and often exceeded galatheid density and abundance in 1992. The major high and low temperature venting areas are indicated in the uppermost graph.

of persistent venting (e.g. at Bio82 and Bio119), individuals of *Tevnia* may have a life-span of 4–5 yr.

The maximum estimated size of *Bathymodiolus thermophilus* individuals surrounding *Riftia* colonies was ∼ 12 cm in November 1995 (4.5 yr after the eruption). According to estimated growth rates for *B. thermophilus* (Rhoads et. al., 1981; Fisher et. al., 1988), this size corresponds to approximately 6.5 yr of age, and thus would have had to colonize these vents late in 1989, 16 months prior to the eruption. Assuming that these mussels were not present in the Transect colonies prior to the eruption, rates of growth exhibited by *B. thermophilus* would be between 2.6 and 11.1 cm/yr — rates considerably higher than those previously estimated for vent-endemic mussels.

Within 2.5 yr of the inception of venting activity, 12 vent-associated species were in the vicinity of newly-formed vents within the Transect area and, after one additional year, 29 species were documented within this same area. In less than 5 yr, the accumulation of 32 species within the Transect accounted for 73% of the total number of species sampled or observed along the length of the 9°–10°N ridge crest (between 9°17′N and 9°54′N) (Table 3). Therefore the establishment of a community typical of those encountered between 9° and 10°N on the EPR required only 3.5 yr. Based on the faunal inventory of Tunnicliffe (1991), approximately 88% of the species inhabiting this region are shared with 13°N EPR, 60% with 21°N EPR, and 42% with vent fields along the Galápagos Rift. At least five taxa encountered between 9°17′N and 9°54′N (12% of taxa found within this region) represent new species (Table 3).

4.2. Patterns of mobile fauna distribution

Comparisons of various mobile vent and non-vent fauna over the entire Transect, mapped from surveys in successive years, revealed that at any given point in time, the distribution of crabs most reflected the spatial distribution of venting activity, with scavenging galatheids favoring dying communities with little H_2S, and predatory brachyurans preferring active areas and vestimentiferan colonies. Similar abundances of nematocarcinid shrimp (*Nematocarcinus ensifer*?) and galatheid crabs along the Transect in March 1992 and December 1993 suggest that these scavengers play a more significant role in the trophic structure of northern EPR hydrothermal vent sites than previously considered. Their tendency to aggregate 5–20 m south of active diffuse venting areas may indicate a general southerly movement of organic material within the ASC. At 13°N EPR, galatheids are believed to preferentially occupy areas close to the *Riftia* thickets (Fustec et al., 1987; Jollivet, 1993). However, our results suggest that these crabs have a lower tolerance to H_2S and/or other reduced chemical species than brachyuran crabs (which are also frequently present on high-temperature vents). It has been shown that *B. thermydron* has a greater resistance to sulfide (no heart rate response up to 1400 μM of sulfide) than both *M. subsquamosa* and *Alvinocaris lusca* (Vetter et al., 1987). We hypothesize that high levels of sulfide in diffuse fluids during the 4 yr following the eruption (Table 3) prevented galatheids from inhabiting their commonly observed habitats within *Tevnia* and *Riftia*

Table 3

Taxonomic list of the 45 species sampled or observed between 9°17′N and 9°54′N along the EPR during cruises associated with this study

Class	Order	Family	Genus	Species
Hydrozoa	Siphonophora	Rhodalidae	*Thermopalia*	*taraxaca*[a]
Anthozoa	Actiniaria	Actinostolidae	*Cyanathea*	*hydrothermala*[a]
Eocanthocephela		Hypoechinorhynchidae	*Hypoechinorhynchus*	*thermaceri*[a]
Obturata	Basibranchia	Riftiidae	*Riftia*	*pachyptila*[a]
		Tevniidae	*Tevnia*	*jerichonana*[a]
			Oasisia	*alvinae*[a]
Polychaeta	Phyllodocida	Polynoidae	*Lepidonotopodium*	*fimbriatum?*[a]
			Branchipolynoe	*symmytilida*
		Hesionidae	*Hesiolyra*	*bergi*[a]
		Nereididae	*Nereis*	sp.[a]
	Terebellida	Ampharetidae	*Amphisamytha*	*galapagensis*[a]
		Alvinellidae	*Alvinella*	*pompejana*[a]
			Alvinella	*caudata*[a]
			Paralvinella	*grasslei*[a]
	Sabellida	Serpulidae	*Laminatubus*	*alvini*[a]
			Protis	*hydrothermica*[a]
Bivalvia	Eulamellibranchia	Vesicomyidae	*Calyptogena*	*magnifica*
	Filibranchia	Mytilidae	*Bathymodiolus*	*thermophilus*[a]
Cephalopoda	Octopoda	Octopodidae	n. gen.	n. sp.[a–c]
Gastropoda	Patellogastropoda	Neolepetopsidae	*Neolepetopsis*	*densata*
			Eulepetopsis	*vitrea*
	Vetigastropoda	Lepetodrilidae	*Lepetodrilus*	*pustulosus*[a]
			Lepetodrilu	*elevatus*[a]
			Lepetodrilu	*cristatus*
			Lepetodrilu	*ovalis*[a]
		Scissurellidae	*Sutilizona*	*theca*
	Neomphalina	Peltospiridae	*Peltospira*	*operculata*
			Peltospira	*delicata*
			Melanodrymia	n. sp.[c]
		Neomphalidae	*Cyathermia*	*naticoides*
	Neotaenioglossa	Provannidae	*Provanna*	sp.
	Caenogastropoda	Turridae	*Phymorrynchus*	sp.[a]
Crustacea	Pedunculata	Scalpellidae	*Neolepas*	sp.
			unidentified gen.	sp.
	Leptostraca	Nebaliidae	*Dahlella*	*caldariensis*[a]
	Copepoda	Siphonostomatoidae	*Aphotopontius*	*acanthinus*[a,c]
	Amphipoda	Pardaliscidae	*Halice*	*hesmonectes*[a,c]
		Lysianassidae	*Ventiella*	*sulfuris*[a]
			n. gen.	n. sp.[a,c]
	Decapoda	Bythograeidae	*Bythograea*	*thermydron*[a]
			Cyanagraea	*praedator*[a]
		Galatheidae	*Munidopsis*	*subsquamosa*[a]
		Bresiliidae	*Alvinocaris*	*lusca*[a]
Pisces	Perciforma	Zoarcidae	*Thermarces*	*andersoni*[a]
		Bythitidae	*Bythites*	*hollisi*[a]

[a] Observed within the Transect.

[b] New species also present at 13°N EPR.

[c] New species.

assemblages. As sulfide levels diminished within the Transect colonies, galatheids moved closer to the vent openings. The increasingly discrete patterns of mobile faunal distribution in time and space stress the importance of investigating temporal changes in vent communities on large continuous spatial scales.

4.3. Influence of vent fluid chemistry

The April 1991 diffuse fluids (22°C to 55°C) contained H_2S concentrations which to date, have only been found in fluids with temperatures exceeding ~ 200°C (Von Damm, 1995). Fluid compositions measured in April 1991 were unusual compared to most diffuse flow because of their low chlorinities, high H_2S concentrations, and high iron and manganese concentrations. For example, a maximum of 0.33 mmol l^{-1} of H_2S was documented (close to the plumes *Riftia*) at the Galápagos Spreading Center (Johnson et al., 1988a), while values of 1–2 mmol kg^{-1} were common at diffuse flow vents associated with the 1991 eruption, and concentrations up to 8.5 mmol kg^{-1} (~ 27 times greater than at Galápagos) were measured at the base of the Tube Worm Pillar (55°C at "Y" vent). Although the absolute H_2S concentrations in diffuse flow vents along the Transect decreased in subsequent years, the absolute levels in November 1995 were still at least twice the maximum of those encountered at the Galápagos Spreading Center (Johnson et al., 1988a). Temperature maxima within the Transect (~ 30°C) also remained twice the maximum of Galápagos vents (e.g. Edmond et al., 1979; Johnson et al., 1986; Johnson et al., 1988a). These unusually high H_2S concentrations in diffuse, low-temperature fluids may provide an explanation for the rapid growth observed within the pioneering colonies of *Tevnia* and *Riftia*. Symbiotic bacteria within the vestimentiferan trophosome may have been influenced by the "abnormally" high levels of H_2S in the diffuse flow, with increased rates of productivity and supported rapid linear worm tube growth (70% faster than any previously reported for *Tevnia*; Roux et al., 1989). The increased surface area of an enlarging trophosome also may have served to support accelerated rates of growth.

Coincidentally, high concentrations of H_2S also may partially explain the lack of colonization by *Riftia* to *Tevnia* colonies in March 1992. While we realize that colonization is a synthesis of many processes, we suggest that *Riftia* larvae may be less tolerant to high levels of H_2S and iron than *Tevnia* larvae, and thus incapable of recruiting to post-eruptive vent areas until the high concentrations of reduced chemicals decrease. A sharp decline of iron was observed over the year following the eruption (Von Damm et al., 1996). Time-series observations within the Transect and at 13° N EPR (Fustec et al., 1987) suggest that the adult form of *Tevnia* may be more tolerant of high hydrothermal flux than adult *Riftia* (perhaps due to differences in plume size and structure). Once *Riftia* was established within the Transect, colonies exhibiting the largest increase in tube worm abundance (e.g., Bio9 and Bio141) also consistently displayed the highest H_2S concentrations.

While there was no detectable migration of hydrothermal activity along the length of transect over 55 months, death of newly formed biological assemblages was either coincident with the cessation of flow or abrupt geochemical changes where low-temperature fluids (29°C) were virtually depleted of H_2S. To the best of our

knowledge, there are only two instances where H$_2$S was considered to be absent from hydrothermal emissions: at one high-temperature vent (291°C) and at several low-temperature vents ($\sim$27°C) on the Juan de Fuca Ridge (Tunnicliffe et al., 1986). However, no vent fauna were directly associated with these venting fluids. The death of the Bio12 colony marks the first time that abrupt changes in vent-fluid geochemistry (loss of H$_2$S and a large increase of iron) have been correlated with the death of a thriving vent community.

4.4. Patterns of faunal colonization

Temporal and spatial patterns of megafaunal colonization represent an intimate relationship between the life-history characteristics of individual species, physical oceanographic processes, and dynamic hydrothermal conditions. Colonization at nascent hydrothermal vents within the Transect suggests a temporal sequence of faunal change that also may be closely connected to changing geochemical conditions. As all vent-endemic fauna ultimately depend on chemosynthesis for their survival, life-history strategies to ensure the persistence of their populations may be directly influenced by changing geochemical conditions. Several other factors may profoundly influence the successional patterns of megafaunal colonization observed at nascent vents within the Transect.

In addition to the influences of fluid chemistry, priority effects, where the conditioning of substrates by microbial alteration or a preceding faunal species, may be a relatively important mechanism for megafaunal colonization. For example, the presence of high microbial production and byproducts may facilitate the early recruitment of some species (e.g. *Tevnia*) and/or preclude the recruitment of other vent-endemic species (e.g. *Riftia* and *Bathymodiolus thermophilus*). If the role of priority effects were a controlling force on the observed pattern of megafaunal colonization, *Riftia* would require some additional biotically mediated cues to settle that are not provided until *Tevnia* sufficiently alters (physically or chemically) the vent microhabitat. However, while the large majority of *Riftia* colonized to thriving *Tevnia* populations, "sporadic" colonization by *Riftia* in many areas where pre-existing *Tevnia* were not present suggests that microhabitat pre-conditioning by *Tevnia* is not mandatory (and perhaps not even relevant). The colonization by *Tevnia* to every area of vigorous venting along the Transect (and not outside these areas) suggests that there may be a causal relationship between *Tevnia* larval recruitment and the earlier presence of microbial material, the particular environmental conditions existing at that time, and larval/symbiont interactions that place aggregates of *Tevnia* close to vent openings.

Species-specific larval recognition and acquisition of the appropriate endosymbiont also may profoundly effect the timing of successful colonization. *Tevnia* and *Riftia* depend on intracellular, sulfur-oxidizing symbiotic bacteria for their energy source. Both *Tevnia* and *Riftia* harbor genetically identical endosymbionts (Edwards and Nelson, 1991) that must be encountered in and ingested from the water column during the worm's larval stage (Jones and Gardiner, 1988; Southward, 1988; Cary et al., 1993). Thus, the procurement of symbionts is prerequisite to the colonization of newly

formed vents. If both *Tevnia* and *Riftia* larvae were present in the water column above the Transect area in April 1991 and March 1992, and colonization of nascent vent areas by *Tevnia* preceded that of *Riftia* in vigorously venting areas, then *Tevnia* larvae may be more efficient with respect to symbiont recognition and/or acquisition than are the larvae of *Riftia. Tevnia* larvae also may be more sensitive to, or tolerant of, high levels of hydrogen sulfide and iron or other physio-chemical constituents than *Riftia.* In contrast, planktotrophic larvae of *B. thermophilus* are thought to acquire their endosymbionts transovarially, from parent to offspring (Cary and Giovannoni, 1993). Thus, one might expect mussel larvae to be one of the earliest colonizers of newly formed vents. The fact that mussels were not observed within the Transect area prior to October 1994 may be due to a combination of our inability to discern extremely small individuals in the video images and the likelihood that they may be relegated to living in cracks or on the underside of the basaltic crust (perhaps in order to avoid potential predators; the underside of basaltic rock samples recovered in October 1994 and November 1995 within the Transect were colonized by numerous mussels less than a 1 cm in length). While symbiont acquisition may impose important constraints that functionally partition recruitment and colonization success of certain vent species over time, these constraints alone do not adequately explain the observed patterns of colonization within the Phoenix vent area.

The sequential appearance of megafaunal species at nascent vents also may be influenced by the distance from larval sources. The distance of larval sources of the dominant megafauna along the 9°–10°N segment to nascent vent areas can be considered to be close (*Riftia*— less than $\sim$ 30 m east, $\sim$ 450 m south, and $\sim$ 700 m to the north; *Tevnia*— $\sim$ 700 m north, $\sim$ 1450 m to the south; and *Bathymodiolus thermophilus*— less than $\sim$ 30 m east, and 430 m to the south). It should be noted that another potential source of larvae were small beds of large vesicomyid clams present 700 m north of the Transect in 1992. *In situ* observations of two spawning episodes by *Riftia* inhabiting the Tube Worm Pillar in November 1992 suggest that these individuals were supplying gametes to the water column (Van Dover, 1994). Given the high levels of inferred long-range dispersal ability for *Riftia* (Black et al., 1994), *Tevnia* (Trivedi et al., 1994), and *B. thermophilus* (Craddock et al., 1995; Jollivet, 1996) along the EPR and the close proximity of these potential larval sources, one might have expected colonization by *Riftia* and *B. thermophilus* to have been concomitant with *Tevnia* at uncolonized newly formed vents.

An alternative source of *Tevnia, Riftia, and B. thermophilus* larvae was the water column overlying the Transect vents between April 1991 and March 1992, where physical oceanographic processes may have temporally partitioned the recruitment and/or colonization success of these three species. Little is known about the dynamic variability of bottom currents and hydrothermal plumes emanating from the ridge crest in this area. From a series of CTD tows near the EPR crest between 9°–10°N, Wijffels et al. (1996) showed that ^{3}He-rich plumes spread westward from the ridge for hundreds of kilometers. Stable periods of moderate bottom flow to the north along the ridge axis followed by abrupt reversals to the south for periods of up to 2 months have been recorded at 13°N EPR in 1991 (Chevaldonné et al., 1997). In contrast, Cannon et al. (1991) showed, in a series of long-term current meter deployments on

the Juan de Fuca Ridge, that the topography of the ridge crest greatly affects the variability in the local current structure. Our observations during hydrocasts conducted to track the hydrothermal plume above the Transect area also suggest large temporal differences in current direction. Buoyant plume surveys conducted between 9°40′N to 9°50′N in December 1991 revealed a notable lack of identifiable vestimentiferan larvae, few mussel and clam larvae (Kim et al., 1994), and large numbers of gastropod larvae (potentially 14 species) (Mullineaux et al., 1996). Hypotheses to explain the temporal partitioning of larvae from correlations of current patterns and relative distance from larval sources are difficult to formulate. However, given that most megafaunal sources of larvae existed within 700 m of the Transect in April 1991, we consider it likely that a pool of *Tevnia*, *Riftia*, and *B. thermophilus* larvae coexisted above the Transect vents immediately following the eruption.

The role of competition and predation as structuring forces in vent community succession remains virtually unexplored. At the Galápagos Rift vents, *Bathymodiolus thermophilus* is thought to outcompete *Riftia* via the removal of hydrogen sulfide from vent fluids prior to the fluid reaching the worm plumes (Johnson *et al.*, 1988b) and through physical displacement of *Riftia* tubes and plumes (Hessler et al., 1988). A recent study suggests that individuals of *Riftia* may be capable of producing an additional connection via tube growth at its posterior end and dissolving its previous attachment to the substrate (Gaill et al., 1997). Thus, *Riftia* may be able to modify its relative position continually to maintain access to vent fluids. This adaptation would yield a competitive advantage over *Tevnia*, which apparently does not possess this capability. Predation by crabs and fish on adult populations of organisms (e.g. amphipods, *Riftia* plumes, and mussels) appeared to have little effect on community composition. However, it is envisioned that predation during the initial stages of community development, through the direct consumption of larvae and juveniles and/or consumption and removal of bacteria or microbial byproducts from the basalt, may have a substantial impact on the subsequent patterns of successful colonization.

In an effort to understand the mechanisms by which the above complex processes interact to produce the sequence of colonization from microbial mats to *Tevnia*, *Riftia*, and *B. thermophilus*, patterns of faunal colonization and the temporal evolution of vent fluid chemistry can be correlated to generate a general descriptive model of low-temperature vent community succession along the fast-spreading EPR between 9°–10°N and contiguous ridge axes. Such models can provide the ecological context for a broad spectrum of manipulative experiments (e.g. Mullineaux et al., 1998), as well as the basis for assessing the impact of a variety of anthropogenic perturbations (e.g. intensive sampling of constituent fauna, drilling of active vent sites, and extraction of polymetallic minerals from accreting hydrothermal deposits) on biological communities at deep-ocean hydrothermal vents.

4.5. Descriptive models of low-temperature hydrothermal vent community succession

The relatively few hypotheses that attempt to explain patterns of succession at deep-sea hydrothermal vents along the northern EPR and Galápagos Rift propose

that as hydrothermal flux and hydrogen sulfide concentrations diminish, bivalves gain a competitive dominance and gradually replace tube worms as the dominant vent megafauna (Hessler et al., 1988). Suspension feeders (e.g. serpulid polychaetes, pectinids, siphonophores, and anemones) decrease with diminishing vent activity, while carnivores (e.g. crabs, shrimp, and whelks) increase in abundance. Mussels are hypothesized to be the last megafaunal survivors as hydrothermal activity ceases at a given vent field.

The model of vent community succession we propose is based on the principle that faunal succession is independent of species availability and assumes availability of a suitable site. Pickett's law of dynamic tolerance (Pickett and Mcdonnell, 1989) states that an assemblage of species having differing tolerances to the abiotic environment and differing capacities for interaction through resource use will sort through time in order of their tolerances. Based on these assumptions, we hypothesize that the following general sequence of biological successional changes occur at deep-sea hydrothermal vents that form after volcanic eruptions along the fast-spreading EPR and contiguous ridge axes.

Shallow dike intrusions, the extrusion of magma onto the seafloor, and the tectonic perturbations associated with submarine eruptions on the MOR crest form the shallow crustal permeability structure through which circulating hydrothermal fluids mix with seawater before exiting the seafloor. This newly formed subsurface network facilitates the potential release of either microbes or microbial byproducts from a subsurface biosphere (a microbial source perhaps latent before the eruption/disturbance) (Deming and Baross, 1993), and creates new habitat space for vent-endemic species. Microbially derived material quickly covers extremely vigorous diffuse vent flow areas of the seafloor in the form of thick white microbial mats. Mobile vent and non-vent fauna (e.g. amphipods, copepods, octopods, brachyuran crabs, galatheid crabs and nematocarcinid shrimp) quickly move in to take advantage of the increase in organic material. Larvae of the pioneering vestimentiferan species, *Tevnia jerichonana*, whether cued by physio-chemical stimuli such as high levels of iron, hydrogen, and/or H_2S, or through efficient acquisition of their endosymbiont from the water column, gregariously settle in the most intense areas of diffuse vent flow, predominantly within primary fissures that served as sites of magma extrusion. Within one year of an eruption, a marked reduction in the areal coverage of the microbial mats will reflect the spatial reduction of hydrothermal flux and the geomorphology of each specific diffuse vent area. The characteristic bulls-eye distribution pattern of vent fauna (Van Dover and Hessler, 1990) will become easily recognizable at each of these individual vent areas by this time, and the gregarious nature of the *Tevnia* settlement will place these founders of discrete colonies at the center of the bulls-eye pattern [a pattern of colonization also observed by Fustec (1987) at 13°N EPR].

Once levels of H_2S and other reduced chemical species have decreased appreciably (within ~ 2 yr) and *Tevnia* colonies are established (~ 30 to 200 ind. per colony), *Riftia*, after acquiring its symbiont from the water column or perhaps near newly established individuals of *Tevnia*, will rapidly grow and dominate all areas containing *Tevnia*, as well as places far removed from intense diffuse flow. The increasing matrix

of *Riftia* tubes will provide microhabitats or refugia for numerous species including amphipods, copepods, shrimp, *Paralvinella grasslei*, and zoarcid fish. *Tevnia* colonization within vestimentiferan colonies will continue, as aggregates of tubes in small tufts. Diffuse vent emissions will become spatially focused over time and any sessile organisms that have colonized these outlying areas will die. As concentrations of H_2S and other reduced chemical species continue to decline (within ~ 3 yr), mussels will begin to colonize the underside of lobate lava crust (perhaps due to their vulnerability to predation as juveniles) and narrow cracks peripheral to diffuse vent openings (meters away). *Riftia* also will colonize peripheral areas inhabited by mussels. Changes in the spatial extent of fluid emissions within a given region will create a patchwork of dead and thriving biological assemblages over time. Mobile fauna will alter their distribution in response to both the spacing of actively venting areas and the location of dead assemblages. Death by cessation of vent flow may occur during any successional stage (and may often occur in less than a year after the initiation of venting). Recently dead assemblages in these areas will be dominated by potentially scavenging colonial siphonophores and galatheid crabs. Galatheid crabs and serpulids will increase in abundance and approach active vent openings as hydrogen sulfide decreases. We hypothesize that galatheids have a limited tolerance to H_2S concentrations that impedes their presence within newly-established faunal colonies. A gradual decrease in H_2S over time will eventually permit them to occupy microhabitats directly on worm tubes at vent openings. Within 4 years of the eruption, galatheids and serpulids will thrive in areas occupied by increasingly dense mussel assemblages that have developed along cracks adjacent to the vestimentiferan colonies. By this time, mussels will be attached to the tubes of *Riftia*.

Based on times-series observations at 13°N EPR (Jollivet, 1993) and the Galápagos Rift (Hessler et al., 1988), we hypothesize that (in the absence of volcanic, tectonic, or anthropogenic disturbance) future observations within the Transect region will reveal that: (1) hydrogen sulfide concentrations will continue to decrease; (2) *Riftia pachyptila* will outcompete and replace *Tevnia jerichonana*; (3) mytilids and vesicomyids will gradually replace the vestimentiferans as the dominant megafauna; and (4) suspension feeders will decrease, and carnivores will increase in abundance. Colonizing mussels will not only outcompete vestimentiferans by displacing their plumes out of the flow, but also by filtering the nutrients from the vent fluids before they can reach the worms' plumes (Johnson et al., 1988b). The continued decrease in vent flux will permit clams to settle in crevices unoccupied by mussels, and in the final waning stages of venting within a vent field, mixotrophic mussels will stand the best chance for survival.

5. Summary and conclusions

Following the 1991 volcanic eruption between 9°45′N and 9°52′N on the East Pacific Rise, time-series observations of community development and associated geochemical conditions in many areas of nascent low-temperature hydrothermal venting were conducted in March 1992, December 1993, October 1994, and November 1995. Much of the erupted volume of the 1991 flow was reimplaced into the

magma plumbing system at shallow crustal levels (manifested as chaotic collapse morphology that dominates the ASC floor and margins from 9°45′–52′N). This process, when coupled with subsequent dike intrusion events within the region, has important implications for the continued heat potential to drive and sustain hydrothermal circulation following an eruption. This geologic setting, and the creation of a circulatory hydrothermal system that develops from it, can evoke a potentially rapid biological response in the form of free-living microbial (and presumably endosymbiotic bacterial) production, which, in turn, supports the structural development and maintenance of dense megafaunal assemblages.

Newly formed low-temperature vent areas were quickly enveloped by large blooms of free-living, sulfur-oxidizing bacteria, potentially derived from a subsurface biosphere. Numerous grazers, scavengers, and predators (e.g. brachyuran and galatheid crabs, zoarcid fish, siphonostomatoid copepods, pardaliscid amphipods, and several species of limpets) rapidly proliferated in response to the large microbial production. Colonization by two symbiont-dependent species of vestimentiferan tube worms was separated in time; pioneering colonies of *Tevnia jerichonana* were established in the most intensely venting areas within eleven months, and populations of *Riftia pachyptila* dominated these same areas 21 months later. Within 3.5 yr, individual *Riftia pachyptila* achieved tube lengths in excess of 2 m, and the increasing density of worm tubes within developing colonies created microhabitats supporting species diversity typical of northern EPR low-temperature vents. At this time, mussels inhabited small basaltic cracks and numerous serpulid polychaetes colonized the periphery of and immediately adjacent to the *Riftia* colonies; one year later small numbers of mussels were fixed directly to the tubes of *Riftia*. Despite the presence of well-established clam communities $\sim$ 700 m north of the Transect area, vesicomyid clams were not observed within any of the newly formed vent areas.

Similar patterns of faunal succession were observed in all areas of persistent low-temperature venting regardless of the distance separating the developing communities, suggesting that these patterns may be predictable. The close proximity of adult megafaunal populations suggests that *Tevnia*, *Riftia*, and *B. thermophilus* larvae were equally available to colonize the Transect vents following the eruption. High levels of iron and H_2S (1.0–2.0 mmol kg^{-1}) were detected in diffuse vent fluid immediately following the 1991 EPR eruption. The steady decline of H_2S and iron observed from April 1991 to November 1995 was coincident with the sequence of vestimentiferan colonization, subsequent mussel colonization, and the encroachment of serpulid polychaetes and galatheid crabs toward vent openings over time.

The observed correlation between patterns of faunal succession and changing geochemical conditions suggests that future models of faunal succession should consider not only the interplay of species-specific life-history strategies, trophic interactions (incorporating estimates of production and biomass), and physical oceanographic processes, but also the effect changing geochemical conditions may have on the sequential colonization of megafaunal species at hydrothermal vents along intermediate to fast-spreading mid-ocean ridges. In addition, the potential for high microbial production and associated abiotic conditions to facilitate the aggregated recruitment of *Tevnia* larvae and/or preclude the recruitment of other sessile

organisms also should be considered in evaluating the underlying controls of community development.

While priority effects, species-specific symbiont acquisition, distances from larval sources, physical oceanographic processes, and competitive/predatory interactions may play important roles in the early assemblage of vent communities, species-specific tolerances to geochemical conditions may also exert community structuring forces responsible for the early recruitment success of *Tevnia* over *Riftia* and the temporal pattern of faunal colonization observed at numerous nascent vents within the Transect. The dynamic interaction of species' life-history strategies, the transient nature of vent habitats, and the variability in geochemical constituents in diffuse hydrothermal fluids (whether serving as larval settlement cues or as barriers to colonization and population growth) play important roles in the adaptation and distribution of vent-endemic species.

Unlike previous attempts to model temporal and spatial changes associated with deep-sea hydrothermal vent communities, our detailed biological and geochemical observations permitted the generation of a robust descriptive model of community succession that takes advantage of (1) the unique opportunity to follow temporal changes in biological community structure and vent fluid geochemistry from the "birth" of numerous deep-sea hydrothermal vents; (2) the increased frequency with which regular repeated observations were documented, and (3) the non-invasive sampling techniques employed to ensure, as much as possible, that the natural development of vent-endemic communities was documented. Colonization exhibited by fauna associated with high-temperature habitats may actively influence the patterns of colonization displayed at low-temperature vents, as these two habitats often share certain species, and may provide refugia or areas of settlement for the other. The incorporation of these patterns into our model in the near future will allow us to develop a more comprehensive understanding of deep-sea hydrothermal vent community development at intermediate to fast-spreading mid-ocean ridges.

Acknowledgements

References

Auzende, J.M., Ballu, V., Batiza, R., Bideau, D., Cormier, M., Fouquet, Y., Geistdoerfer, P., Lagabrielle, Y., Sinton, J., Spadea, P., 1994. Activité magmatique, tectonique et hydrother-male actuelle sur la Dorsale Est Pacifique entre 17° et 19° (campagne NAUDUR). Comptes Rendus Academic Sciences Paris, 319, Série II, 811–818.

Black, M.B., Lutz, R.A., Vrijenhoek R.C., 1994. Gene flow among vestimentiferan tube worm (Riftia pachyptila) populations from hydrothermal vents of the eastern Pacific. Marine Biology 120, 33–39.

Buckland, S.T., Anderson, D.R., Burnham, K.P., Laake, J.L., 1993. Distance Sampling: Estimating Abundance of Biological Populations. Chapman & Hall, London.

Bush, M.B., Whittaker, R.J., 1991. Krakatau: colonization patterns and hierarchies. Journal of Biogeography 18, 341–356.

Cannon, G.A., Pashinski, D.J., Lemon, M.R., 1991. Middepth flow near hydrothermal venting sites on the southern Juan de Fuca Ridge. Journal of Geophysical Research 96, 1 2815–12 831.

Carbotte, S.M., MacDonald, K.C., 1992. East Pacific Rise 8°–10°30′N: evolution of ridge segments and discontinuities from SeaMARC II and three-dimensional magnetic studies. Journal of Geophysical Research 97 (3569), 6959–6982.

Cary, S.C., Giovannoni, S.J., 1993. Transovarial inheritance of endosymbiotic bacteria in clams inhabiting deep-sea hydrothermal vents and cold seeps. Proceedings National Academy of Sciences 90, 5695–5699.

Cary, S.C., Warren, W., Anderson, E., Giovannoni, S.J., 1993. Identification and localization of bacterial endosymbionts in hydrothermal vent taxa with symbiont-specific polymerase chain reaction amplification and in situ hybridization techniques. Molecular Marine Biology and Biotechnology 2, 51–62.

Chevaldonné, P., Godfroy, A., Guezennec, J., Lesongeur, F., Fouquet, Y., Barbier, G., Desbruyères, D., 1995. InterRidge, 4, 15–16.

Chevaldonné, P. Jollivet, D., Vangriesheim, A., Desbruyères, D., 1997. Hydrothermal-vent alvinellid polychaete dispersal in the eastern Pacific: I. Influence of vent site distribution, bottom currents, and biological patterns. Limnology and Oceanography 42, 67–80.

Childress, J.J., Fisher, C.R., 1992. The biology of hydrothermal vent animals: physiology, biochemistry, and autotrophic symbioses. Oceanographical Marine Biology Annual Review 30, 337–441.

Connell, J.H., 1979. Tropical rain forests and coral reefs as open non-equilibrium systems. In: Population Dynamics. Anderson, R.M., Turner, B.D., Taylor, L.R., (Ed.). Blackwell, Oxford pp. 141–163.

Craddock, C., Hoeh, W.R., Gusfatson, R.G., Lutz, R.A., Hashimoto, J., Vrijenhoek, R.C., 1995. Evolutionary relationships among deep-sea mytilids (Bivalvia: Mytilidae) from hydrothermal vents and cold-water methane/sulfide seeps. Marine Biology 124, 137–146.

Dale, V.H., 1991. Mount St. Helens; revegetation of Mount St. Helens debris avalanche 10 years post eruption. National Geographic Research and Exploration 7, 328–341.

Delaney, J.R., Embley, R.W., 1993. An October response cruise to the June-July intrusive/eruptive events at the CoAxial segment of the Juan de Fuca Ridge. EOS, Transactions of American Geophysical Union 75, 617.

Deming, J.W., Baross, J.A., 1993. Deep-sea smokers: windows to a subsurface biosphere? Geochimica et Cosmochimica Acta N°Sp 57, 3219–3230.

Diamond, J.M., 1994. Pitcairn before the Bounty. Nature 369, 608.

Doumenc, D., Van-Praët, M., 1988. Actinies abyssales d'un site hydrothermal du Pacifique oriental. Oceanological Acta, N°Sp 8, 61–68.

Duennebier, F.K., Becker, N.C., Caplan-Auerbach, J., Clague, D.A., Cowan, J., Cremer, M., Garcia, M., Goff, F., Malahoff, A., McMutry, G.M., Midson, B.P., Moyer, C.L., Norman, M., Okubo, P., Resing, J.A., Rhodes, J.M., Rubin, K., Sansone, F.J., Smith, J.R., Spencer, K., Wen, X., Wheat, C.G., 1997. Researchers rapidly respond to submarine activity at Loihi Volcano, Hawaii. EOS, Transactions of American Geophysical Union, 78, 229–233.

Edmond, J.M., Measures, C., Mangum, B., Grant, B., Sclater, F.R., Collier, R., Hudson, A., Gordon, L.L., Corliss, J.B., 1979. Ridge crest hydrothermal activity and the balances of the major and minor elements in the ocean: the Galápagos data. Earth and Planetary Science Letters 46, 19–30.

Edwards, D.B., Nelson, D.C., 1991. DNA-DNA solution hybridization studies of the bacterial symbionts of hydrothermal vent tube worms (Riftia pachyptila and Tevnia jerichonana). Applied and Environmental Microbiology 57, 1082–1088.

Embley, R.W., Chadwick, W.W., Jonasson, I.R., Butterfield, D.A., Baker, E.T., 1995. Initial results of the rapid response to the 1993 CoAxial event: relationships between hydrothermal and volcanic processes. Geophysical Research Letters 22, 143–146.

Embley, R.W., Chadwick, W.W., Shank, T., Christie, D., 1996. Geology of the 1996 Gorda Ridge eruption from analysis of multibeam, towed camera, sidescan, and ROV data. EOS, Transactions of American Geophysical Union 77(46), F1.

Fisher, C.R., Childress, J.J., Arp, A.J., Brooks, J.M., Distel, D., Favuzzi, J.A., Felbeck, H., Hessler, R.R., Johnson, K.S., Kennicutt, M.C., II., Macko, S.A., Newton, A., Powell, M.A., Somero, G.M., Soto, T., 1988. Microhabitat variation in the hydrothermal vent mussel, Bathymodiolus thermophilus, at the Rose Garden vent on the Galápagos Rift. Deep-Sea Research 35, 1769–1791.

Fornari, D.J., Haymon, R.M., Edwards, M.H., Macdonald. K.C., 1990. Volcanic and tectonic characteristics of the East Pacific Rise crest 9°09′N to 9°54′N: Implications for fine-scale segmentation of the plate boundary. EOS, Transactions of American Geophysical Union 71, 625.

Fornari, D.J., Van Dover, C.L., Shank, T.M., Lutz, R.A., Olsson, M., 1994. A versatile, low-cost temperature sensing device for time-series measurements at deep-sea hydrothermal vents. Bridge Newletter 6, 37–40.

Fornari, D.J., Embley, R.W., 1995. Tectonic and volcanic controls on hydrothermal processes at the Mid-Ocean Ridge: an overview based on near-bottom and submersible studies. In: Physical, Chemical, Biological, and Geological Interactions within Sea-floor Hydrothermal Systems, Geophysical Monograph 91. Humphris, S.E., Zierenberg, R.A., Mullineaux, L., Thomson, R., (Eds.), American Geophysical Union, Washington, DC., pp. 1–46.

Fornari, D.J., Haymon, R.M., Perfit, M.R., Gregg, T.K.P., Edwards, M.H, 1998. Axial Summit Caldera of the East Pacific Rise 9°N to 10°N: Geologic characteristics and evolution of the axial zone on fast-spreading mid-ocean ridges. Journal of Geophysical Research (in press).

Fridriksson, S., Magnusson, B., 1989. Development of an ecosystem on Surtsey with references to Anak Krakatau. GeoJournal 28, 287–291.

Fustec, A., Desbruyères, D., Juniper, S.K., 1987. Deep-sea hydrothermal vent communities at 13°N on the East Pacific Rise: Microdistribution and temporal variations. Biology and Oceanography 4, 121–164.

Gaill, F., Shillito, B., Ménard, F., Goffinet, G., Childress, J.J., 1997. Rate and process of tube worm production by the deep-sea hydrothermal vent tube worm Riftia pachyptila. Marine Ecology Progress Series 148, 135–143.

Geistdoerfer, P., Auzende, J.M., Batiza, R., Bideau, D., Cormier, M., Fouquet, Y., Lagabrielle, Y., Sinton, J., Spadea, P., 1995. Hydrothermalisme et communautés animales associées sur la dorsale du Pacifique oriental entre 17°S et 19°S (campagne Naudur, décembre 1993). Comptes Rendus Academic Sciences Paris 320, Série IIa, 47–54.

Grassle, J.F., 1985. Distribution and biology of hydrothermal vent animals. Science 229, 713–717.

Gregg, T.K.P., Fornari, D.J., Perfit, M.R., Haymon, R.M., Fink, J.H., 1996. Rapid emplacement of a mid-ocean ridge lava flow on the East Pacific Rise at 9°46′–51′N. Earth and Planetary Science Letters 144, E1–E7.

Haymon, R.M., Fornari, D.J., Edwards, M.H., Carbotte, S., Wright, D., Macdonald, K.C., 1991. Hydrothermal vent distribution along the East Pacific Rise Crest (9°09′–54′N) and its relationship to magmatic and tectonic processes on fast-spreading mid-ocean ridges. Earth and Planetary Science Letters 104, 513–534.

Haymon, R.M., Fornari, D.J., Von Damm, K.L., Lilley, M.D., Perfit, M.R., Edmond, J.M., Shanks, W.C., III, Lutz, R.A., Grebmeier, J.M., Carbotte, S., Wright, D., McLaughlin, E., Smith, M., Beedle, N., Olson, E., 1993. Volcanic eruption of the mid-ocean ridge along the East Pacific Rise crest at 9°45–52′N: Direct submersible observations of seafloor phenomena associated with an eruption event in April, 1991. Earth and Planetary Science Letters 119, 85–101.

Hessler, R.R., Smithey, W.M., 1983. The distribution and community structure of megafauna at the Galápagos Rift hydrothermal vents. In: Rona, P.A., Boström, K., Laubier, L., Smith, J.K.L., (Eds.), Hydrothermal Processes at Seafloor Spreading Centers. Plenum Press, New York, pp. 735–770.

Hessler, R.R., Smithey, W.M., Keller, C.H., 1985. Spatial and temporal variation of giant clams, tubeworms and mussels at deep-sea hydrothermal vents. Biological Society of Washington Bulletin 6, 465–474.

Hessler, R.R., Smithey, W.M., Boudrias, M.A., Keller, C.H., Lutz, R.A., Childress, J.J., 1988. Temporal change in megafauna at the Rose Garden hydrothermal vent (Galápagos Rift; eastern tropical Pacific). Deep-Sea Research 35, 1681–1709.

Hessler, R.R., Desbruyères, D., 1991. Contrasting patterns of temporal changes at hydrothermal vents between the EPR at 13°N and Rose Garden on the Galapagos Rift, Sixth Deep-Sea Biology Symposium, Copenhagen, p. 36.

Holden, C., 1996. Oceanographers make their own hot springs. Science 274, 349.

Humes, A.G. Lutz, R.A., 1994. Aphotopontius acanthinus, new species (copepoda: siphonostomatoida), from deep-sea hydrothermal vents on the East Pacific Rise. Journal of Crustacean Biology 142, 337–345.

Johnson, H.P., Tunnicliffe, V., 1988. Time lapse photography of a hydrothermal system: A successful one-year deployment. EOS, Transactions of American Geophysical Union 69, 1024–1026.

Johnson, K.S., Beehler, C.L., Sakamoto-Arnold, C.M., Childress, J.J., 1986. In situ measurements of chemical distributions in a deep-sea hydrothermal vent. Science 231, 1139–1141.

Johnson, K.S., Childress, J.J., Beehler, C.L., 1988a. Short-term temperature variability in the Rose Garden hydrothermal vent field: an unstable deep-sea environment. Deep-Sea Research 35, 1711–1721.

Johnson, K.S., Childress, J.J., Hessler, R.R., Sakamoto-Arnold, C.M., Beehler, C.L., 1988b. Chemical and biological interactions in the Rose Garden hydrothermal vent field, Galapagos spreading center. Deep-Sea Research 35, 1723–1744.

Jollivet, D., 1993. Distribution et évolution de la faune associée aux sources hydrothermales profondes à 13°N sur la dorsale du Pacifique oriental: le cas particulier des polychètes Alvinellidae. Thèse de doctorat nouveau régime, Université de Bretagne Occidentale, pp. 357.

Jollivet, D., 1996. Specific and genetic diversity at deep-sea hydrothermal vents: an overview. Biodiversity and Conservation 5, 1619–1653.

Jones, M.L., Gardiner, S.L., 1988. Evidence for a transient digestive tract in Vestimentifera. Proceedings of the Biological Society of Washington 101, 423–433.

Kaartvedt, S., Van Dover, C.L., Mullineaux, L.S., Wiebe, P.H., Bollens, S.M., 1994. Amphipods on a deep-sea hydrothermal treadmill. Deep-Sea Research 41, 179–195.

Keough, M.J., 1984. Dynamics of the epifauna of the bivalve pinna-bicolor: interactions among recruitment, predation, and competition. Ecology 65, 677–688.

Kim, S., Mullineaux, L.S., Helfrich, K.R., 1994. Larval dispersal via entrainment into hydrothermal vent plumes. Journal of Geophysical Research 99, 12 655–12 665.

Lilley, M.D., Olson, E.J., McLaughlin, E.A., Von Damm, K.L., Bray, A.M., Buttermore, L.G., 1996. The geochemical relationship between high temperature hydrothermal vents and directly adjacent diffuse flow sites. EOS, Transactions of American Geophysical Union 77(46), F404.

Lutz, R.A., Fritz, L.W., Cerrato, R.M., 1988. A comparison of bivalve (Calyptogena magnifica) growth at two deep-sea hydrothermal vents in the eastern Pacific. Deep-Sea Research 35, 1793–1810.

Lutz, R.A., 1991. Sixth Deep-Sea Biology Symposium, Copenhagen, October 1991.

Lutz, R.A., Shank, T.M., Fornari, D.J., Haymon, R.M., Lilley, M.D., Von Damm, K.L., Desbruyères, D., 1994. Rapid growth at deep-sea vents. Nature 371, 663–664.

Martin, J.W., France, S.C., Van Dover, C.L., 1993. Halice hesmonectes, a new species of pardaliscid amphipod (Crustacea, Peracarida) from hydrothermal vents in the eastern Pacific. Canadian Journal Zoology 71, 1724–1732.

Massoth, G.J., Milburn, H.B., Hammond, S.R., Butterfield, D.A., McDuff, R.E., Lupton, J.E., 1988. The geochemistry of submarine venting fluids at Axial Volcano, Juan de Fuca Ridge: new sampling methods and a VENTS program rational. In: DeLuca, M.P., Babb, I., (Eds.), Global Venting, Midwater, and Benthic Ecological Processes, NURP Research Report 88-4, 29–59.

McCormick, M.I., Choat, J.H., 1987. Estimating total abundance of a large temperate-reef fish using visual strip-transects. Marine Biology 96, 469–478.

Milligan, B.N., Tunnicliffe, V., 1994. Vent and nonvent faunas of Cleft segment, Juan de Fuca Ridge, and their relations to lava age. Journal of Geophysical Research 99, 4777–4786.

Mullineaux, L.S., Kim, S.L., Pooley, A., Lutz, R.A., 1996. Identification of archaeogastropod larvae from a hydrothermal vent community. Marine Biology 124, 551–560.

Mullineaux, L.S., Mills, S.W., Goldman, E., 1998. Recruitment variation during a pilot study of hydrothermal vents (9°50′N, East Pacific Rise). Deep-sea Research II 45(1–3), 441–464.

Nelson, D., 1991. Rapid growth of unusual hydrothermal bacteria observed at new vents during ADVENTURE dive program to the EPR crest at 9°45′–52′N. EOS, Transactions of American Geophysical Union 72, 481.

Oosting, S.E., Von Damm, K.L., 1996. Bromide/chloride fractionation in seafloor hydro-
thermal fluids from 9°–10°N East Pacific Rise. Earth and Planetary Science Letters 144,
133–145.

Pickett, S.T.A., White, P.S., (Eds.), 1985. The Ecology of Natural Disturbance and Patch
Dynamics. Academic Press, Orlando, FL.

Pickett, S.T.A., McDonnell, M.J., 1989. Changing perspectives in community dynamics: a
theory of successional forces. Trends in Evolution and Ecology 4, 11–14.

Rhoads, D.C., Lutz, R.A., Revelas, E.C., Cerrato, R.M., 1981. Growth of bivalves at deep-sea
hydrothermal vents along the Galapagos Rift. Science 214, 911–913.

Roux, M., Rio, M., Schein, E., Lutz, R.A., Fritz, L.W., Ragone, L.M., 1989. Mesures in situ de la
croissance des bivalves et des vestimentifères et de la corrosion des coquilles au site
hydrothermal de 13°N (dorsale du Pacifique oriental). Comptes Rendus Academic Science
Sér. III, 308, 121–127.

Shank, T.M., Fornari, D.J., Von Damm, K.L., Lilley, M.D., Van Dover, C.L., Lévai, G., Lutz,
R.A., 1995. Dynamic fluctuations and cyclic periodicities of low-T hydrothermal venting;
time-lapse multi-probe temperature measurements and video imaging at 9°49.8′N on the
East Pacific Rise- results from December 1993 to October 1995. EOS, Transactions of
American Geophysical Union 76, 701.

Sousa, W.P., 1980. The responses of a community to disturbance: the importance of suc-
cessional age and species' life histories. Oecologia 45, 72–81.

Southward, E.C., 1988. Development of the gut and segmentation of newly settled stages of
Ridgeia (Vestimentifera): implications for relationship between Vestimentifera and Pogono-
phora. Journal of the Marine Biological Association of U.K. 68, 465–487.

Thornton, I.W.B., Walsh, D., 1992. Photographic evidence of rate of development of plant cover
on the emergent island Anak Krakatau from 1971 to 1991 and implications for the effect of
volcanism. Geojournal 28.2, 249–259.

Trivedi, A.K., Black, M.B., Vrijenhoek, R.C., 1994. Allozyme diversity within and among tube
worm (vestimentiferan) species from deep-sea hydrothermal vents of the east pacific rise.
Isozyme Bulletin 23, 47.

Tunnicliffe, V., 1990. Observations on the effects of sampling on hydrothermal vent habitat and
fauna of Axial Seamount, Juan de Fuca Ridge. Journal of Geophysical Research 95,
12 961–12 966.

Tunnicliffe, V., 1991. The biology of hydrothermal vents: ecology and evolution. Oceanography
and Marine Biology Annual Review 29, 319–407.

Tunnicliffe, V., Botros, M., DeBurgh, M.E., Dinet, A., Johnson, H.P., Juniper, S.K., McDuff,
R.E., 1986. Hydrothermal vents on Explorer Ridge, northeast Pacific. Deep-Sea Research
33, 401–412.

Tunnicliffe, V., Garrett, J., Johnson, H.P., 1990. Physical and biological factors affecting the
behavior and mortality of hydrothermal vent tubeworms (vestimentiferans). Deep-Sea
Research 37, 103–125.

Tunnicliffe, V., Juniper, S.K., 1990. Dynamic character of the hydrothermal vent habitat and the
nature of sulphide chimney fauna. Progress in Oceanography 24, 1–13.

Tunnicliffe, V., Embley, R.W., Holden, J.F., Butterfield, D.A., Massoth, G.J., Juniper, S.K., 1998.
Biological colonization of new hydrothermal vents following an eruption on Juan de Fuca
Ridge. Deep-Sea Research 44, 1627–1644.

Tusting, R., Davis, D., 1992. Laser systems and structured illumination for quantitative
undersea imaging. Marine Technology Society Journal 26 (4), 5–12.

Tusting, R., Davis, D., 1993. Improved methods for visual and photographic benthic surveys.
Proceedings of Diving for Science-93, AAUS, pp. 157–172.

Van Dover, C.L., Hessler, R.R., 1990. Spatial variation in faunal composition of hydrothermal vent communities on the East Pacific Rise and Galápagos spreading center. In: McMurray, G.R., (Ed.), Gorda Ridge: A Seafloor Spreading Center in the United States' Exclusive Economic Zone, Springer, New York, pp. 253–264.

Van Dover, C.L., Kaartvedt, S., Bollens, S.M., Wiebe, P.H., Martin, J.W., France, S.C., 1992. Deep-sea amphipod swarms. Nature 358, 25–26.

Van Dover, C.L., 1994. In situ spawning of hydrothermal vent tubeworms (Riftia pachyptila). Biological Bulletin 186, 134–135.

Vetter, R.D., Wells, M.E., Kurtsman, A.L., Somero, G.N., 1987. Sulfide detoxification by the hydrothermal vent crab Bythograea thermydron and other decapod crustaceans. Physiological Zoology 60(1), 121–137.

Von Damm, K.L., Oosting, S.E., Buttermore, L.G., 1994. Chemical evolution of diffuse hydrothermal fluids from $9°49'–50'N$ EPR: The BIOTRANSECT area, EOS, Transactions of American Geophysical Union 75, 601.

Von Damm, K.L., 1995. Controls on the chemistry and temporal variability of seafloor hydrothermal fluids, In: Humphris, S.E., Zierenberg, R.A., Mullineaux, L., Thomson, R., (Eds.), Physical, Chemical, Biological, and Geological Interactions within Seafloor Hydrothermal Systems, Geophysical Monograph 91, American Geophysical Union pp. 222–247.

Von Damm, K.L., Bray, A.M., Buttermore, L.G., Lilley, M.D., 1996. Chemical changes between high temperature and diffuse flow fluids at $9°\ 50'N$ East Pacific Rise. EOS, Transactions of American Geophysical Union 77, 403–404.

Von Damm, K.L., Buttermore, L.G., Oosting, S.E., Bray, A.M., Fornari, D.J., Lilley, M.D., Shanks III, W.C., 1997. Direct observation of a high-temperature vent from vapor to brine. Earth and Planetary Science Letters 149, 101–111.

Watremez, P., Kervévan, C., 1990. Origine des variations de l'activité hydrothermale: premiers éléments de réponse d'un modèle numérique simple. Comptes Rendus Academie Sciences Paris, Sér. II 311, 153–158.

Wijffels, S.E., Toole, J.M., Bryden, H.L., Fine, R.A., Jenkins, W.J., Bullister, J.L., 1996. The water masses and circulation at $10°N$ in the Pacific. Deep-Sea Research 43, 501–544.

Wright, D.J., Haymon, R.M., Fornari, D.J., 1995. Crustal fissuring and its relationship to magmatic and hydrothermal processes on the East Pacific Rise crest ($9°12'N$ to $54'N$). Journal of Geophysical Research 100, 6097–6120.